

STEADY-ACE : A Computer Program  
for Three-Dimensional Nuclear and  
Thermal-Hydraulic Analysis of BWR Core

---

March 1980

---

日本原子力研究所

Japan Atomic Energy Research Institute

## JAERI レポート

この報告書は、日本原子力研究所で行われた研究および技術の成果を研究成果編集委員会の審査を経て、不定期に刊行しているものです。

### 研究成果編集委員会

委員長 石川 寛 (理事)

#### 委員

赤石 準 (保健物理部)	田中 正俊 (核融合研究部)
朝岡 卓見 (原子炉工学部)	仲本秀四郎 (技術情報部)
今井 和彦 (環境安全研究部)	長崎 隆吉 (燃料工学部)
神原 忠則 (材料試験炉部)	橋谷 博 (原子炉化学部)
小林 岩夫 (動力試験炉部)	浜口 由和 (物理部)
栗山 将 (高崎研究所)	原 昌雄 (動力炉開発・安全性研究管理部)
佐々木吉方 (研究炉管理部)	原田吉之助 (物理部)
佐藤 一男 (安全解析部)	更田豊治郎 (企画室)
佐野川好母 (高温工学室)	三井 光 (高崎研究所)
四方 英治 (製造部)	森島 淳好 (安全工学部)

入手 (資料交換による)、複製などの問合わせは、日本原子力研究所技術情報部 (〒319-11 茨城県那珂郡東海村) まで、お申しこみください。なお、このほかに財団法人原子力弘済会資料センター (茨城県那珂郡東海村日本原子力研究所内) で複写による実費頒布をおこなっております。

## JAERI Report

Published by the Japan Atomic Energy Research Institute

### Board of Editors

Hiroshi Ishikawa (Chief Editor)

Jun Akaishi	Masao Hara	Isamu Kuriyama	Yoshikata Sasaki
Takumi Asaoka	Kichinosuke Harada	Hiroshi Mitsui	Kazuo Sato
Toyojiro Fuketa	Kazuhiko Imai	Atuyoshi Morishima	Konomo Sanokawa
Yoshikazu Hamaguchi	Masanori Kanbara	Ryukichi Nagasaki	Eiji Shikata
Hiroshi Hashitani	Iwao Kobayashi	Hideshiro Nakamoto	Masatoshi Tanaka

Inquiries about the availability of reports and their reproduction should be addressed to the Division of Technical Information, Japan Atomic Energy Research Institute, Tokai-mura, Naka-gun, Ibaraki-ken, Japan.

編集兼発行 日本原子力研究所  
印刷 三美印刷株式会社

# A Computer Program for Three-Dimensional Nuclear and Thermal-Hydraulic Analysis of BWR Core : STEADY-ACE

Yoshitaka NAITO, Kiyoharu ABE, Mitsuru MAEKAWA\*

Division of JPDR

Tokai Research Establishment  
Japan Atomic Energy Research Institute,  
Tokai-mura, Naka-gun, Ibaraki-ken

Received June 14, 1979

A FORTRAN computer program named as STEADY-ACE has been developed to predict the three-dimensional distributions of neutron flux, power and void fraction in a BWR core. The program consists of two subprograms, i.e., the few-group three-dimensional diffusion subprogram DIFFUSION-ACE and the thermal-hydraulic subprogram HYDRO-ACE. The two subprograms are combined in an iterative way so that the interdependency of the power distribution and the void fraction distribution can be treated consistently.

The program STEADY-ACE provides a prediction of BWR core performance in a good accuracy in a reasonably short computation time. The computation time of the example case of JPDR quarter core (72/4 assemblies) is 7 CPU minutes on the machine FACOM 230-75.

Keywords : Computer Program, STEADY-ACE, Core Performance, BWR, JPDR, DIFFUSION-ACE, Three Dimension, Power Distribution, Neutron Diffusion, HYDRO-ACE, Multi-Channel, Thermal-Hydraulics, Void Fraction Distribution, Two Phase Flow, Leakage Iterative Method.

---

\* General Electric Technical Services Co. Inc.

## BWR 炉心 3次元核熱水力計算プログラム： STEADY-ACE

内藤 俣 孝, 阿部 清 治, 前川 充 留\*

日本原子力研究所東海研究所動力試験炉部

1979年6月14日 受理

計算機用プログラム STEADY-ACE は、BWR 炉心内の3次元中性子束、出力および減速材ボイド体積割合の空間分布を計算により求めるために開発された。このプログラムは2つのサブプログラムからなっている。即ち、少数群3次元拡散方程式を解くプログラム DIFFUSION-ACE と熱水力計算プログラム HYDRO-ACE の2つである。この2つのサブプログラムは、出力分布とボイド分布の相関性が矛盾なく取り扱えるように、繰り返し計算の形で結合されている。

プログラム STEADY-ACE は、実用的な範囲の少ない計算機時間で BWR の炉心特性を精度良く計算する。例を挙げるならば、72 燃料集合体よりなる JPDR の 1/4 炉心の場合の計算時間は、計算機 FACOM-230-75 で CPU 時間で7分間である。

## Contents

1. Introduction .....	1
2. Geometry .....	2
3. Basic Equations .....	6
3.1 Basic Equations in HYDRO-ACE .....	6
3.2 Basic Equations in DIFFUSION-ACE .....	11
3.3 Interfaces between HYDRO-ACE and DIFFUSION-ACE .....	15
4. Input Description .....	18
5. Major Output .....	28
5.1 Print-out .....	28
5.2 Punched Cards .....	28
6. Numerical Examples .....	29
6.1 Sample Input and Output of STEADY-ACE .....	29
6.2 Power Distribution in JPDR-II Core .....	29
6.3 Coolant Flow Distribution in JPDR-II Core .....	31
7. Conclusion .....	33
Acknowledgement .....	33
References .....	33
Appendix A STEADY-ACE Sample Input .....	34
Appendix B STEADY-ACE Sample Output .....	35

## 目 次

1. 序 論	1
2. 幾何形状の表現	2
3. 基 礎 式	6
3.1 HYDRO-ACE のための基礎式	6
3.2 DIFFUSION-ACE のための基礎式	11
3.3 HYDRO-ACE と DIFFUSION-ACE の結合方式	15
4. 入力形式	18
5. 主要計算出力形式	28
5.1 プリント出力	28
5.2 パンチカード出力	28
6. 計 算 例	29
6.1 STEADY-ACE の例題の入力および出力データ	29
6.2 JPDR-II 炉心の出力分布	29
6.3 JPDR-II 炉心の冷却材流量配分	31
7. 結 論	33
謝 辞	33
参考文献	33
付録 A STEADY-ACE の例題の入力データ	34
付録 B STEADY-ACE の例題の出力データ	35

## 1 Introduction

One of the objectives in the BWR core design is to verify that the power peaking factor does not exceed the limiting value. It is therefore very important to calculate the power peaking factor accurately.

The difficulties in the calculation of the power peaking factor are: (1) the power distribution is skewed both horizontally and vertically due to the insertion of the control rods and (2) the void fraction distribution and the power distribution are so strongly dependent on each other that they cannot be calculated separately. Three-dimensional calculation is required to overcome the first difficulty. The second difficulty can be solved by performing the iterative calculation between the thermal-hydraulic calculation to get the void fraction distribution and the neutron diffusion calculation to obtain the power distribution.

A number of computer programs have been developed to solve these difficulties. The commonly used program is FLARE<sup>1)</sup>, which has an advantage of short computation time, but also a disadvantage of low accuracy. One of the causes for its low accuracy is that the power distribution calculation is based on the pseudo-diffusion equation using the neutron transport kernel. Another cause is that the flow rate distribution in the flow channels is given apriori by the separate thermal-hydraulic calculations, such as by JP-HYDRO<sup>2)</sup> or HYDRO-ACE<sup>3)</sup>. The interdependency of the void fraction and power distributions cannot be treated by FLARE in a satisfactory manner. A computer program named as STEADY-ACE satisfying these requirements has been developed to overcome the disadvantages of FLARE.

The program STEADY-ACE combines the two computer programs; the thermal-hydraulic program HYDRO-ACE and the three-dimensional neutron diffusion program DIFFUSION-ACE<sup>4)</sup>, to treat the interdependency of the void fraction and the power distributions more accurately. HYDRO-ACE calculates the flow rates and the void distributions in the flow channels in the core shroud. DIFFUSION-ACE adopts a new method called "Leakage Iterative Method"<sup>5)</sup> to solve the three-dimensional diffusion equation of two or three energy groups to obtain the power distribution. The new method is one of the synthesis methods which combine the  $z$ -directional one-dimension calculation with the  $x$ - $y$  directional two-dimensional calculation. The computation time can be reduced significantly by the "Leakage Iterative Method" without sacrificing the accuracy. The advantage of short computation time in DIFFUSION-ACE allows the practical use of the void-power iteration in STEADY-ACE.

## 2 Geometry

STEADY-ACE simulates a BWR core performance. The calculational model in STEADY-ACE is explained here using an example of the JPDR-II core. JPDR is a small BWR located in Tokai Research Establishment of Japan Atomic Energy Research Institute. The reactor has been modified since 1964 to double the power capacity. The modified reactor is called as JPDR-II. The major core parameters of JPDR-II are given in TABLE 2.1. The  $x$ - $y$  cross section of the JPDR-II core is illustrated in Fig. 2.1.

The calculational model of a BWR core for the thermal-hydraulic calculation HYDRO-ACE is discussed first. A BWR core, such as JPDR-II core, consists of parallel channels. As each fuel assembly is enclosed by a channel box, each flow path in a channel box can be treated separately to predict its thermal-hydraulic behaviors. The flow paths outside the channel boxes are treated collectively as one flow path named as "leakage flow channel". The leakage flow channel includes the flow paths between the channel boxes in the dummy fuel assemblies and near the surrounding core shroud. Figure 2.2 shows the horizontal view of the JPDR-II core model for the thermal-hydraulic calculation. The flow paths are numbered, taking the symmetry into consideration. The example of JPDR-II core in Fig. 2.2 is based on its 90 degree mirror symmetry. This numbering sequence is arbitrary except the leakage flow channel should have the last number.

The vertical model of each flow channel is given in Fig. 2.3. The flow channel is divided into a number of sections based on the flow area and thermal characteristics. The heated zone is treated separately from the unheated zone. In the example of Fig. 2.3, the flow channel is divided into 6 sections, i.e., lower supporter, nose piece, lower unheated zone, heated zone, upper unheated zone and upper supporter. The heated zone is divided equally further into "block".

TABLE 2.1 JPDR-II core data

(1) Fuel rod		(4) Control rod	
Pellet diameter	10.66 mm	Number	16
Clad thickness	0.70 mm	Type	cross-shaped section
Clad outer diameter	12.23 mm	Pitch (square array)	273.2 mm
Fuel effective length	1,467 mm	Stroke	about 150 cm
Gas plenum volume	13 cc	Width	225.4 mm
Fuel material	UO <sub>2</sub>	Effective length	1,460 mm
Clad material	Zr-4	Poison	B <sub>4</sub> C powder
Fuel density	10.41 g/cc	Clad & sheath material	S. S.
(2) Fuel assembly		Width of follower	114.3 mm
Number of fuel assembly	72	Thickness of follower	6.35 mm
Fuel rod array	7×7	Effective length of Follower	1,283 mm
Number of fuel rods per assembly	49	Follower material	Zr-4
Fuel rod pitch	16.6 mm	B <sub>4</sub> C density	70%
UO <sub>2</sub> weight per assembly	1370×49 kg	(5) Poison curtain	
Fuel assembly weight	about 100 kg	Number	24
(3) Channel box		Type	flat board
Thickness	1.5 mm	Width	2.48 mm
Material	Zr-4	Thickness	3.2 mm
		Length	1,667 mm
		Poison	Boron in SS
		Boron concentration	1,030 ppm



The blocks are numbered sequentially from the bottom to the top. The elevation of the blocks should be equal for all of the flow channels.

Next, the calculational model of a BWR core for the nuclear calculation DIFFUSION-ACE is discussed. A BWR core is divided into square lattice cells of fuel bundles as shown in Fig. 2.4. The nuclear cross sections associated with the lattice cells are defined to be the homogenized nuclear cross sections for the fuel, cladding, channel box, interior water, exterior water, (if applicable) control rods and poison curtains. The fuel bundle cells are designated by the same number as the thermal-hydraulic model described earlier in this section. The regions outside the fuel bundles are called collectively as "side reflector". The number assigned to the side reflector is 0, as shown in Fig. 2.4. The cross sections associated with the side reflector are often assumed to be the cross sections of water without steam voids.

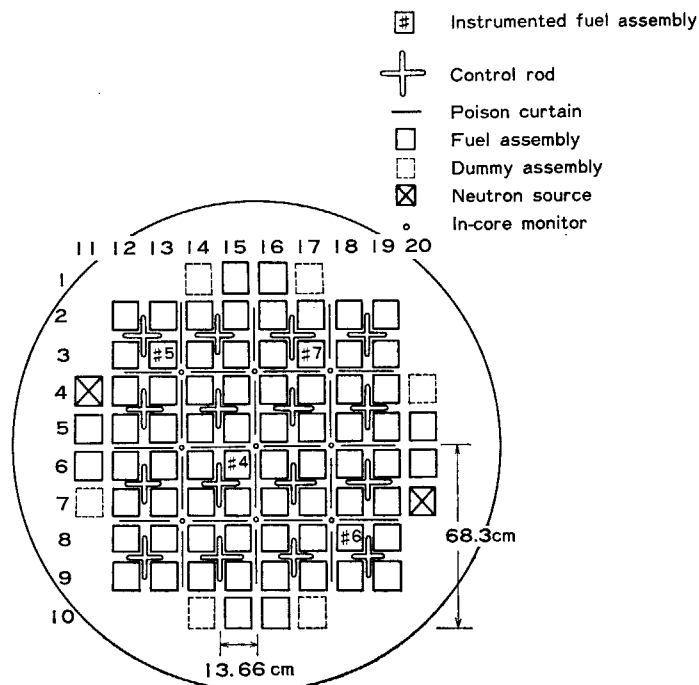


Fig. 2.1 X-Y cross section of JPDR-II core

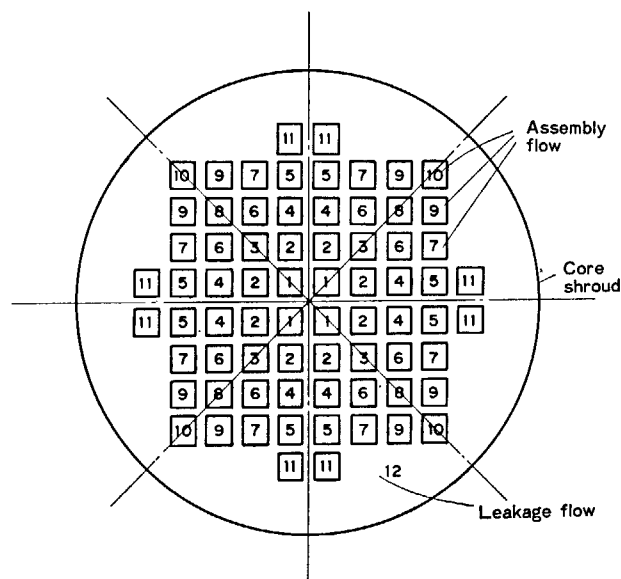


Fig. 2.2 Horizontal geometry for HYDRO-ACE

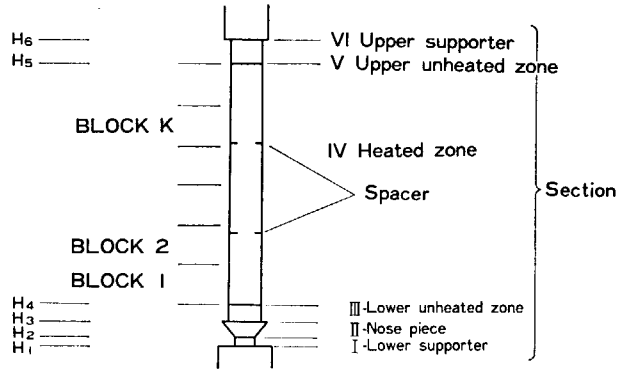


Fig. 2.3 Vertical geometry for HYDRO-ACE

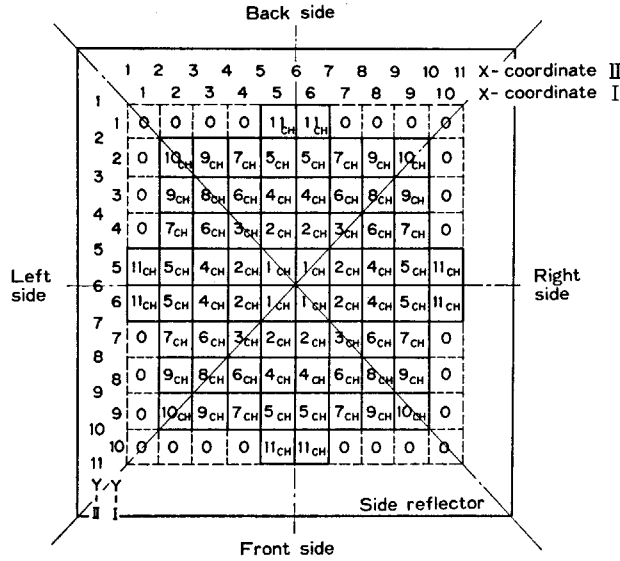


Fig. 2.4 Horizontal geometry for DIFFUSION-ACE

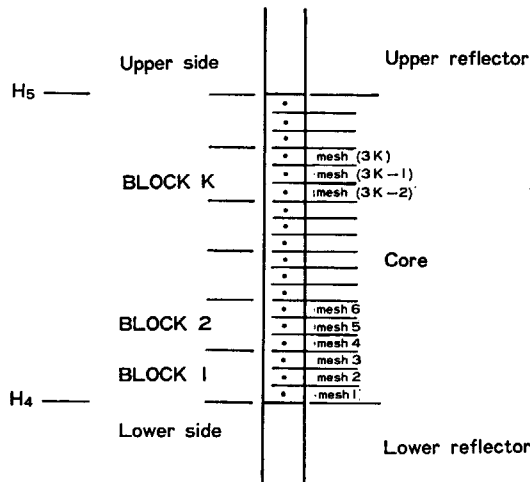


Fig. 2.5 Vertical geometry for DIFFUSION-ACE

The fuel bundle cells are also called as channels in this report. But there is a minor difference between the channels in the thermal-hydraulic model and the channels in the nuclear model. The channels in the nuclear model include the water between the channel boxes, control rods and poison curtains, but the channels in the thermal-hydraulic model do not. The water between the channel boxes is included in the leakage flow path in the thermal-hydraulic model.

The vertical geometry for nuclear calculation is shown in **Fig. 2.5**. The channel is divided into 3 regions. The region corresponding to the heated zone in the thermal-hydraulic model is now called as "core" in the nuclear model. The lower regions including lower unheated zones, nose piece and lower supporter in **Fig. 2.3** are called collectively as "lower reflector" in **Fig. 2.5** and assumed to be homogeneous in the nuclear properties. In other words, uniform cross sections are assigned to the lower reflector region. Similarly, the upper regions including the upper unheated zone and upper supporter in **Fig. 2.3** are called collectively as "upper reflector" in **Fig. 2.5** and assumed to be homogeneous in the nuclear properties.

The "core" region is further divided into blocks in the same way as discussed in the thermal-hydraulic model. The size, elevation and identification number of the blocks in the nuclear model should be identical to those in the thermal-hydraulic model. As the blocks of the same identification number are at the same elevation, they form a layer between the two horizontal parallel planes. In other words, a block is a parallel-piped defined by a channel and a layer.

The program DIFFUSION-ACE solves the three-dimensional diffusion equation by solving alternatively one-dimensional equation for each of the channels and two-dimensional equation for each of the layers. In order to improve the accuracy of calculations, blocks are further subdivided into meshes. For example, in the one-dimensional calculation for each of the channels, blocks are subdivided into meshes, as shown by the example in **Fig. 2.5**. The objective of the subdivision into meshes is to make the mesh size length comparable to the diffusion length of thermal neutrons. Similarly, a block is subdivided into a few meshes in the x and y directions in the two-dimensional diffusion calculation for each of the layers.

Finally, the coordinates in the x-y horizontal cross section are discussed. Two coordinate systems are used as shown in **Fig. 2.4**. X-coordinate I (or Y-coordinate I) is used to designate the channel location and x-coordinate II (or Y-coordinate II) is used to designate the locations of the control rods and the in-core monitors.

### 3 Basic Equations

STEADY-ACE is composed of the thermal-hydraulic subprogram HYDRO-ACE and the three-dimensional neutron diffusion subprogram DIFFUSION-ACE. The basic equations of the two subprograms and their interface are explained in this chapter.

#### 3.1 Basic Equations in HYDRO-ACE

HYDRO-ACE calculates the flow rates and the void distributions in the flow channels in the core shroud. The power distributions in the channels are supplied from DIFFUSION-ACE.

The flow rates in the flow channels are determined so that the pressure differentials between the inlets and outlets are equal for all of the flow channels. The pressure differentials consist of head loss, friction loss, expansion/contraction loss, spacer loss and acceleration loss.

The head loss is expressed by the following equation.

$$\begin{aligned}\Delta P_H &= \int_{Z_{in}}^{Z_{out}} \rho(z) dz \\ &= \int_{Z_{in}}^{Z_L} \rho(z) dz + \int_{Z_L}^{Z_u} \rho(z) dz + \int_{Z_u}^{Z_{out}} \rho(z) dz \\ &= \rho_{in} \cdot (Z_L - Z_{in}) + \sum_{k=1}^K \rho_k \Delta Z + \rho_{k+1} \cdot (Z_{out} - Z_u),\end{aligned}\quad (3.1)$$

where

$\Delta P_H$ : head loss [kg/m<sup>2</sup>]

$Z_{in}$ : height of the inlets of the flow channels [m]

$Z_{out}$ : height of the outlets of the flow channels [m]

$Z_L$ : height of the lower end of the heated zone [m]

$Z_u$ : height of the upper end of the heated zone [m]

$\rho_k$ : fluid density at the  $k$ -th block [kg/m<sup>3</sup>]

$\rho_{k+1}$ : fluid density at the upper end of the heated zone [kg/m<sup>3</sup>]

$\rho_{in}$ : fluid density at the inlet

$\Delta Z$ : length of one block

$K$ : number of the blocks.

The friction loss depends on the flow characteristic, i.e. single phase flow or two phase flow. The friction loss for single phase flow is expressed by

$$\begin{aligned}\Delta P_{FR} &= f \cdot \frac{\rho}{2g} V^2 \frac{dz}{De} \\ &= f \cdot \frac{W^2}{2g \cdot \rho \cdot A^2} \cdot \frac{dz}{De},\end{aligned}\quad (3.2)$$

where

$\Delta P_{FR}$ : single phase friction loss [kg/m<sup>2</sup>]

$f$ : friction factor

$\rho$ : density [kg/m<sup>3</sup>]

$g$ : gravitational acceleration [9.8 m/sec<sup>2</sup>]

$V$ : velocity [m/sec]

$De$ : equivalent hydraulic diameter [m]

$dz$ : length [m]

$W$ : mass flow rate [kg/sec]

$A$ : flow area [m<sup>2</sup>].

The friction factor  $f$  is non-dimensional and expressed as  $f$  function of the Reynolds number  $Re$ :

For  $Re < 2000$  (laminar flow)

$$f = \frac{64}{Re}, \quad (3.3)$$

For  $2000 < Re < 10^4$  (Blasius' equation)

$$f = 0.3164 Re^{-0.25}, \quad (3.4)$$

For  $10^4 < Re < 1.9 \times 10^6$  (Hermann's equation)

$$f = 0.00540 + 0.397 \cdot Re^{-0.3}, \quad (3.5)$$

$Re$  is defined as

$$Re = \frac{De \cdot W}{\rho \cdot A \cdot \nu}, \quad (3.6)$$

where  $\nu$ : viscosity [m<sup>2</sup>/sec].

The friction loss for two phase flow has been studied by a number of researchers. HYDRO-ACE allows the user to select an equation from the following four correlations.

#### Martinelli-Nelson correlation

$$\Delta P_{\text{TPF}} = \phi_{\text{lt}} \cdot \Delta P_l, \quad (3.7)$$

where

$\Delta P_{\text{TPF}}$ : two phase friction loss

$\phi_{\text{lt}}$ : two phase friction multiplier

$$\Delta P_l = f \cdot \frac{W_l^2}{2g \cdot \rho_l \cdot A^2} \cdot \frac{dz}{De},$$

$\rho_l$ : density of liquid

$W_l$ : flow rate of liquid phase

$$W_l = W_o \cdot (1 - x) \quad (3.8)$$

$W_o$ : total flow rate

$x$ : quality

The local two phase friction multiplier  $\phi_{\text{lt}}$  is expressed as a function of the quality and the absolute pressure, as shown in Fig. 3.1.

#### Sher's correction

Sher proposed a correction of Martinelli-Nelson correlation. Figure 3.2 gives the two phase friction multiplier as a function of the mass flow rate and quality based on Westinghouse data. Figure 3.3 shows the relative value of the two phase friction multiplier to the value at  $G = 10^6$  (lb/hr·ft<sup>2</sup>).

#### Armand's correlation

Armand's correlation is based on the total flow rate rather than the liquid phase rate.

$$\Delta P_{\text{TPF}} = R_o \cdot \Delta P_o, \quad (3.9)$$

where

$\Delta P_{\text{TPF}}$ : two phase friction loss

$R_o$ : two phase friction multiplier

$$\Delta P_o = f \cdot \frac{W_o^2}{2g \cdot \rho_l \cdot A^2} \cdot \frac{dz}{De}.$$

The two phase friction multiplier is expressed as

$$R_o = \begin{cases} (1-\alpha)^{-1.42} & \text{for } 0 \leq \alpha \leq 0.65 \\ 0.478(1-\alpha)^{-2.2} & \text{for } 0.65 < \alpha \leq 0.9 \\ 1.73(1-\alpha)^{-1.64} & \text{for } 0.9 < \alpha \leq 0.999 \end{cases} \quad (3.10)$$

where  $\alpha$  is a void fraction.

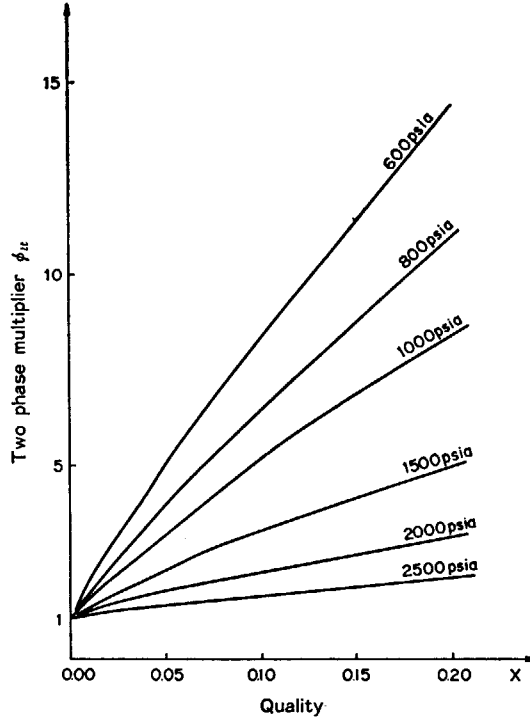


Fig. 3.1 Two phase flow friction loss multiplier by Martinelli-Nelson.

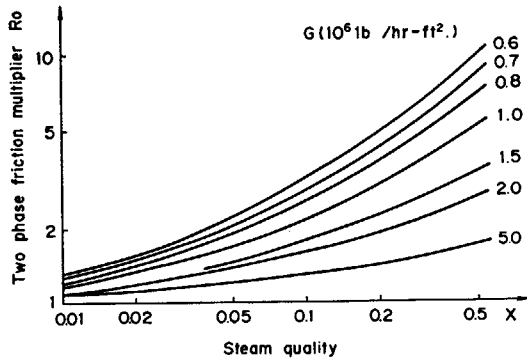


Fig. 3.2 Westinghouse two phase friction multiplier by Sher.

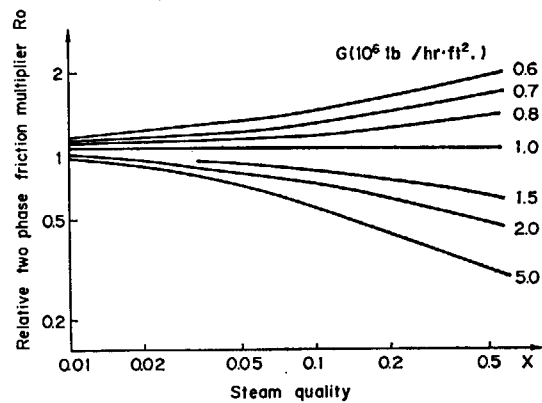


Fig. 3.3 Two phase friction loss multiplier normalized to that of  $10^6 \text{ lb/hr-ft}^2$  (Sher's method).

**Lottes-Finn's correlation**

Lottes-Finn's correlation is similar to Armand's correlation. The difference lies in the expression of the two phase friction multiplier. It is expressed as

$$R_o = \left( \frac{1-x}{1-\alpha} \right)^2 \quad (3.11)$$

The pressure loss due to the change of the flow area is called  $E/C$  pressure loss in this document (see Fig. 3.4). For expansion flow, the pressure loss is expressed as

$$\Delta P_{E/C} = K_{E/C} \cdot \frac{\rho}{2g} V_1^2 \quad (3.12)$$

For contraction flow, it is expressed as

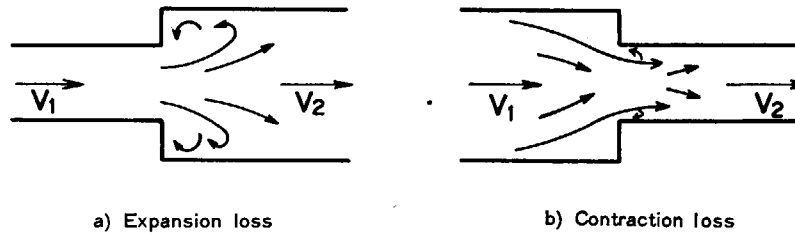


Fig. 3.4 Model for calculating expansion contraction loss.

TABLE 3.1 Relation of contraction rate  $A_2/A_1$  and loss coefficient  $K_{E/C}$ .

$A_2/A_1$	0.10	0.20	0.30	0.40	0.50	0.60	0.70	0.80	0.90
$K_{E/C}$	0.48	0.45	0.41	0.36	0.29	0.21	0.13	0.07	0.01

$$\Delta P_{E/C} = K_{E/C} \cdot \frac{\rho}{2g} V_1^2, \quad (3.13)$$

where

$\Delta P_{E/C}$ : E/C pressure loss

$K_{E/C}$ : E/C loss coefficient

$\rho$ : average density at the location of flow area change [ $\text{kg/m}^3$ ]

$g$ : gravitational acceleration [ $9.8 \text{ m/sec}^2$ ]

$V_1$ : velocity before flow area change [ $\text{m/sec}$ ]

$V_2$ : velocity after flow area change [ $\text{m/sec}$ ].

The E/C loss coefficient  $K_{E/C}$  is determined by the Weisbach's method. For expansion flow,

$$K_{E/C} = \left(1 - \frac{A_1}{A_2}\right)^2, \quad (3.14)$$

$A_1$ : flow area before change [ $\text{m}^2$ ]

$A_2$ : flow area after change [ $\text{m}^2$ ].

For contraction flow the coefficient is derived by the interpolation between the values in TABLE 3.1.

The spacer pressure loss is estimated by

$$\Delta P_{sp} = K_{sp} \cdot \frac{\rho}{2g} V^2, \quad (3.15)$$

$\Delta P_{sp}$ : pressure loss due to spacer [ $\text{kg/m}^2$ ]

$K_{sp}$ : spacer pressure loss coefficient

$\rho$ : average density at spacer location [ $\text{kg/m}^3$ ]

$g$ : gravitational acceleration ( $=9.8 \text{ m/sec}^2$ )

$V$ : average velocity of the two phase flow [ $\text{m/s}$ ].

Finally, the acceleration loss is estimated by

$$\Delta P_{acc} = \frac{W}{g} (V_{out} - V_{in}), \quad (3.16)$$

$\Delta P_{acc}$ : acceleration loss [ $\text{kg/m}^2$ ]

$W$ : mass flow rate [ $\text{kg/sec}$ ]

$g$ : gravitational acceleration ( $=9.8 \text{ m/sec}^2$ )

$V_{in}$ : inlet flow velocity [ $\text{m/s}$ ]

$V_{out}$ : outlet flow velocity [ $\text{m/s}$ ]

In the pressure loss calculations described above, the important variables are enthalpy, steam quality and void fraction. The estimation of these variables is discussed below.

The enthalpy is calculated as

$$H(z) = H_{in} + \frac{q(z)}{W}, \quad (3.17)$$

$H(z)$ : enthalpy at a given position  $z$  [kcal/kg]

$H_{in}$ : inlet enthalpy [kcal/kg]

$q(z)$ : heat generated in the fuel bundle from inlet up to the position  $z$  [kcal/sec]

$W$ : mass flow rate in the bundle [kg/sec].

The quality is calculated as

$$x(z) = \frac{H(z) - H_t}{H_g - H_t}, \quad (3.18)$$

$x(z)$ : quality at the position  $z$

$H(z)$ : enthalpy at the position  $z$  [kcal/kg]

$H_t$ : enthalpy of saturated water [kcal/kg]

$H_g$ : enthalpy of saturated steam [kcal/kg].

The void fraction is estimated by the Maurer's method<sup>(6)</sup> for three different regions.

**Region 1**: Subcooled region

**Region 2**: Transition region from Region 1 to Region 3

**Region 3**: Bulk boiling region

The boundary of the above three regions are:

**Boundary between Region 1 and Region 2**: The average thickness of the steam film on the heated surface is 0.004 inch.

**Boundary between Region 2 and Region 3**: The void fraction is 40%.

The void fraction correlation for the above three regions is as follows:

**Region 1**

The heat transfer coefficient at the heated surface is estimated by

$$h = 0.030 \frac{K}{De} (Re)^{0.8} (Pr)^{0.4}, \quad (3.19)$$

$h$ : heat transfer coefficient [Btu/hr·ft<sup>2</sup>·°F]

$k$ : thermal conductivity of water [Btu/hr·ft·°F]

$De$ : hydraulic diameter [ft]

$Re$ : Reynolds number

$Pr$ : Prandtl number.

The wall temperature of the heated surface  $T_w$  is estimated by

$$T_w = T_{sat} + 60 \cdot \left(\frac{q}{10^6}\right)^{0.25} \cdot \exp\left[-\left(\frac{P}{90}\right)\right], \quad (3.20)$$

where  $T_w$ : wall temperature [°F]

$T_{sat}$ : saturation temperature of water [°F]

$q$ : heat flux [Btu/hr·ft<sup>2</sup>]

$P$ : system pressure [psia].

The thickness of the steam film,  $a$  [ft] is calculated from the heat transfer coefficient  $h$  and the wall temperature as

$$a = \frac{[q - h(T_w - T_B)] \cdot Pr \cdot K}{1.07 \cdot h^2 \cdot (T_{sat} - T_B)}, \quad (3.21)$$

where  $a$ : thickness of the steam film [ft]

$T_B$ : temperature corresponding to the bulk enthalpy at the given position [°F].

The thickness  $a$  is described by the MKS unit system as

$$a' = 0.3048 \cdot a, \quad (3.22)$$

$a'$ : thickness of the steam film [m].

Then the void fraction is calculated as

$$\alpha = a' \cdot l_H / A, \quad (3.23)$$



$\alpha$ : void fraction

$l_H$ : heated circumferential [m]

$A$ : flow area [m<sup>2</sup>].

The Eq. (3.23) is applicable for  $a \leq 0.004/12$  ft ( $a' \leq$  about 0.1 mm).

### Region 2

The void fraction in Region 2 is calculated by the interpolation of the enthalpy.

$$\alpha = \alpha_1 + (\alpha_3 - \alpha_1) \frac{H - H_1}{H_3 - H_1}, \quad (3.24)$$

$\alpha$ : void fraction for a given enthalpy  $H$

$H_1$ : enthalpy at the end point of Region 1, i.e.  $a = 0.004/12$  ft

$\alpha_1$ : void fraction at the end point of Region 1

$\alpha_3$ : 0.40 (starting point of Region 3)

$H_3$ : enthalpy at the starting point of Region 3, i.e.  $\alpha_3 = 0.40$ .

### Region 3

The void fraction is calculated by the Bankoff's equation.

$$\alpha = \frac{0.71 + 10^{-4} \cdot P}{1 + \frac{\rho_g}{\rho_l} \cdot \frac{1-x}{x}}, \quad (3.25)$$

$\alpha$ : void fraction

$P$ : system pressure

$\rho_g$ : density of saturated steam [kg/m<sup>3</sup>]

$\rho_l$ : density of saturated water [kg/m<sup>3</sup>]

$x$ : quality.

## 3.2 Basic Equations in DIFFUSION-ACE

DIFFUSION-ACE solves a three-dimensional diffusion equation by combining the  $z$ -directional one-dimension and the  $x$ - $y$ -directional two dimension calculations. A new method called "Leakage Iterative Method" has been developed to perform the alternating one-dimensional and two-dimensional calculations effectively.

A general diffusion equation is

$$\nabla D \nabla \phi - \Sigma_T \phi + S = 0, \quad (3.26)$$

where  $D$ : diffusion coefficient

$\phi$ : neutron flux

$\Sigma_T = \Sigma_a + \Sigma_r$

$\Sigma_a$ : absorption cross section

$\Sigma_r$ : slowing down cross section

$S$ : source.

Integrating Eq. (3.26) over a block which is assumed to be homogeneous in its nuclear characteristics, we get

$$\begin{aligned} & D \int_{\Delta x} \int_{\Delta y} \int_{\Delta z} dx dy dz \left( \frac{\partial^2 \phi}{\partial x^2} + \frac{\partial^2 \phi}{\partial y^2} \right) + D \int_{\Delta x} \int_{\Delta y} \int_{\Delta z} dx dy dz \left( \frac{\partial^2 \phi}{\partial z^2} \right) \\ & - \Sigma_T \int_{\Delta x} \int_{\Delta y} \int_{\Delta z} \phi dx dy dz + \int_{\Delta x} \int_{\Delta y} \int_{\Delta z} S dx dy dz = 0, \end{aligned} \quad (3.27)$$

where  $\Delta x$ ,  $\Delta y$  and  $\Delta z$  give the dimensions of the block.

The leakage terms  $L_{xy}$  and  $L_z$  are defined as

$$-L_{xy} = \frac{D \int_{\Delta x} \int_{\Delta y} \int_{\Delta z} \left( \frac{\partial^2 \phi}{\partial x^2} + \frac{\partial^2 \phi}{\partial y^2} \right) dx dy dz}{\int_{\Delta x} \int_{\Delta y} \int_{\Delta z} \phi dx dy dz} \quad (3.28)$$

$$-L_z = \frac{D \int_{\Delta x} \int_{\Delta y} \int_{\Delta z} \left( \frac{\partial^2 \phi}{\partial z^2} \right) dx dy dz}{\int_{\Delta x} \int_{\Delta y} \int_{\Delta z} \phi dx dy dz} \quad (3.29)$$

The flux and source terms integrated over a block are given as

$$\phi_b = \int_{\Delta x} \int_{\Delta y} \int_{\Delta z} \phi dx dy dz, \quad (3.30)$$

$$\theta_b = \int_{\Delta x} \int_{\Delta y} \int_{\Delta z} S dx dy dz. \quad (3.31)$$

Inserting Eqs. (3.28), (3.29), (3.30) and (3.31) into Eq. (3.27), it gives

$$-(L_{xy} + L_z + \Sigma_T) \phi_b + \theta_b = 0. \quad (3.32)$$

Given  $\theta_b$ ,  $L_{xy}$ ,  $L_z$  and  $\Sigma_T$ , the integrated flux  $\phi_b$  can be easily derived from Eq. (3.32). But the leakage terms  $L_{xy}$  and  $L_z$  are not given a priori. The leakage terms  $L_{xy}$  and  $L_z$  must be derived from the two-dimensional calculations and the one-dimensional calculations, respectively.

Let  $\phi_z$  and  $\theta_z$  be defined as

$$\phi_z = \int_{\Delta x} \int_{\Delta y} \phi dx dy, \quad (3.33)$$

$$\theta_z = \int_{\Delta x} \int_{\Delta y} S dx dy. \quad (3.34)$$

Rearranging Eq. (3.27) as follows:

$$D \int_{\Delta z} dz \int_{\Delta x} \int_{\Delta y} \left( \frac{\partial^2 \phi}{\partial x^2} + \frac{\partial^2 \phi}{\partial y^2} \right) dx dy + D \int_{\Delta z} dz \frac{\partial^2}{\partial z^2} \int_{\Delta x} \int_{\Delta y} \phi dx dy - \Sigma_T \int_{\Delta z} dz \int_{\Delta x} \int_{\Delta y} \phi dx dy + \int_{\Delta z} dz \int_{\Delta x} \int_{\Delta y} S dx dy = 0, \quad (3.35)$$

and rewriting Eq. (3.35) by the use of the definitions given by Eqs. (3.33) and (3.34), i.e.,

$$-L_{xy} \int_{\Delta z} \phi_z dz + D \int_{\Delta z} \frac{\partial^2 \phi_z}{\partial z^2} dz - \Sigma_T \int_{\Delta z} \phi_z dz + \int_{\Delta z} \theta_z dz = 0, \quad (3.36)$$

we get finally,

$$D \frac{\partial^2 \phi_z}{\partial z^2} - (L_{xy} + \Sigma_T) \phi_z + \theta_z = 0. \quad (3.37)$$

Given  $L_{xy}$  for each block,  $\phi_z$  can be derived by solving the one-dimensional equation (3.37). The leakage term  $L_z$  is then derived from  $\phi_z$ . From the definition of  $L_z$ , Eq. (3.29) is rewritten as

$$D \int_{\Delta z} \frac{\partial^2 \phi_z}{\partial z^2} dz = -L_z \int_{\Delta z} \phi_z dz. \quad (3.38)$$

Inserting Eq. (3.38) into Eq. (3.36),

$$-L_z \int_{\Delta z} \phi_z dz - L_{xy} \int_{\Delta z} \phi_z dz - \Sigma_T \int_{\Delta z} \phi_z dz + \int_{\Delta z} \theta_z dz = 0. \quad (3.39)$$

Then  $L_z$  is given as

$$L_z = \frac{\int_{\Delta z} \theta_z dz}{\int_{\Delta z} \phi_z dz} - (\Sigma_T + L_{xy}). \quad (3.40)$$

Given  $L_z$ , the  $x$ - $y$  directional leakage term  $L_{xy}$  is then similarly calculated from two-dimensional calculation.

Next we derive the  $x$ - $y$  dimensional diffusion equation. Let  $\phi_{xy}$ ,  $\theta_{xy}$  be defined as

$$\phi_{xy} \equiv \int_{\Delta z} \phi dz, \quad (3.41)$$

$$\theta_{xy} \equiv \int_{\Delta z} S dz. \quad (3.42)$$

Reformulating Eq. (3.27) in the same way as performed in deriving Eq. (3.37), i.e.,

$$\begin{aligned} & D \int_{\Delta x} \int_{\Delta y} dx dy \left( \frac{\partial^2}{\partial x^2} + \frac{\partial^2}{\partial y^2} \right) \cdot \left( \int_{\Delta z} \phi dz \right) \\ & + D \int_{\Delta x} \int_{\Delta y} dx dy \int_{\Delta z} \left( \frac{\partial^2 \phi}{\partial z^2} \right) dz \\ & - \Sigma_T \int_{\Delta x} \int_{\Delta y} dx dy \int_{\Delta z} \phi dz + \int_{\Delta x} \int_{\Delta y} dx dy \int_{\Delta z} S dz = 0, \end{aligned} \quad (3.43)$$

$$\begin{aligned} & D \int_{\Delta x} \int_{\Delta y} dx dy \left( \frac{\partial^2}{\partial x^2} + \frac{\partial^2}{\partial y^2} \right) \phi_{xy} - L_z \int_{\Delta x} \int_{\Delta y} \phi_{xy} dx dy \\ & - \Sigma_T \int_{\Delta x} \int_{\Delta y} \phi_{xy} dx dy + \int_{\Delta x} \int_{\Delta y} \theta_{xy} dx dy = 0, \end{aligned} \quad (3.44)$$

we have

$$D \left( \frac{\partial^2}{\partial x^2} + \frac{\partial^2}{\partial y^2} \right) \phi_{xy} - (L_z + \Sigma_T) \phi_{xy} + \theta_{xy} = 0. \quad (3.45)$$

Given  $L_z$  for each block,  $\phi_{xy}$  is calculated by solving the two-dimensional equation (3.45).  $L_{xy}$  is then to be derived from  $\phi_{xy}$ . From the definition of  $L_{xy}$  in Eq. (3.28), the following relation is derived,

$$D \int_{\Delta x} \int_{\Delta y} \left( \frac{\partial^2}{\partial x^2} + \frac{\partial^2}{\partial y^2} \right) \phi_{xy} dx dy = -L_{xy} \int_{\Delta x} \int_{\Delta y} \phi_{xy} dx dy. \quad (3.46)$$

Inserting Eq. (3.46) into Eq. (3.44), we get

$$\begin{aligned} & -L_{xy} \int_{\Delta x} \int_{\Delta y} \phi_{xy} dx dy - L_z \int_{\Delta x} \int_{\Delta y} \phi_{xy} dx dy \\ & - \Sigma_T \int_{\Delta x} \int_{\Delta y} \phi_{xy} dx dy + \int_{\Delta x} \int_{\Delta y} \theta_{xy} dx dy = 0. \end{aligned} \quad (3.47)$$

$L_{xy}$  is then given as

$$L_{xy} = \frac{\int_{\Delta x} \int_{\Delta y} \theta_{xy} dx dy}{\int_{\Delta x} \int_{\Delta y} \phi_{xy} dx dy} - (L_z + \Sigma_T). \quad (3.48)$$

The leakage terms  $L_{xy}$  and  $L_z$  are derived from Eqs. (3.48) and (3.40) respectively, but  $L_{xy}$  (and  $L_z$ ) should be given to get  $L_z$  ( $L_{xy}$ , vice versa). Then an iterative calculation is necessary to get  $L_{xy}$  and  $L_z$ .

The iterative calculations are performed as described in the following. Given initial guess of  $L_{xy}$  for each block, the one-dimensional calculation solving Eq. (3.37) is performed for each of the channel. The blockwise  $z$ -directional leakage term  $L_z$  is then calculated by Eq. (3.40). Given the value of  $L_z$  for each block, the two-dimensional calculation solving Eq. (3.45) is performed for each of the horizontal layer. The blockwise  $x$ - $y$  directional leakage  $L_{xy}$  is then calculated by Eq. (3.48). The iterative calculations are performed until the consistency is achieved between  $L_{xy}$  and  $L_z$ . The convergence of the iteration is determined by comparing the following two quantities with each other.

$$(\phi_b)_z = \int_{\Delta x} \int_{\Delta y} \phi_z dx dy, \quad (3.49)$$

$$(\phi_b)_{xy} = \int_{\Delta z} \phi_{xy} dz. \quad (3.50)$$

If  $L_{xy}$  and  $L_z$  have consistency, the following relation should be satisfied ;

$$\phi_b = (\phi_b)_z = (\phi_b)_{xy}. \tag{3.51}$$

The neutron balance is obtained by the iteration discussed above, which corresponds to the inner iteration in the finite difference calculation.

The advantage of the Leakage Iterative Method is to allow subdivisions of the blocks in the one-dimensional and/or two-dimensional calculations. The coarse mesh, such as 1 mesh point in an assembly (1/2 foot width), makes the finite difference method less accurate than desired, because the diffusion length of thermal neutrons in light water is less than the mesh width. As one-dimensional calculations and two-dimensional calculations are performed separately, the subdivisions of the blocks provide a desired accuracy in solving the diffusion equation without increasing the computation time significantly.

Another remarkable feature of DIFFUSION-ACE is the treatment of the reflector regions. In general, a large number of mesh points is assigned to the reflector regions because the thermal neutron flux have a peak in the reflector region, which increases the computation time and capacity requirement dramatically. In order to avoid assigning mesh points to the reflector regions, a new boundary condition has been developed by us. In the core region, the flux is determined by the finite difference method but in the reflector region, the flux is derived analytically. At the boundary between the core region and the reflector region, the continuities of the neutron current and the neutron flux are assumed. This approach is called here as "analytical boundary condition."

The approach is explained here by the example of one-dimensional geometry illustrated in Fig. 3.5.

In the reflector regions the one-dimensional diffusion equation is expressed as

$$\frac{d^2}{dr^2}\phi - k^2\phi = 0, \tag{3.52}$$

where  $k^2 = (\Sigma_{TR} + D_R B^2) / D_R, \tag{3.53}$

$D_R$  : diffusion coefficient in the reflector region

$\Sigma_{TR}$  : total cross section in the reflector region

$B^2$  : buckling of neutron flux

The differential equation (3.52) is solved on the conditions :

$$\begin{aligned} \phi_R &= \phi_{B1} && \text{at } r=0, \\ \phi_R &= 0 && \text{at } r=+\infty, \end{aligned}$$

where B1 refers to the boundary shown in Fig. 3.5. The solution of Eq. (3.52) is given by

$$\phi(r) = \phi_{B1} \cdot e^{-kr} \tag{3.54}$$

The continuity of the neutron current at the boundary is expressed as

$$-\left(-D_R \left(\frac{d\phi}{dr}\right)_{r=0}\right) = -D_1 \cdot \frac{\phi_1 - \phi_{B1}}{\left(\frac{\Delta z_1}{2}\right)}, \tag{3.55}$$

where the subscript 1 refers to the first mesh point in the core region. The left hand side of Eq. (3.55) is calculated from Eq. (3.54) as

$$D_R \left(\frac{d\phi}{dr}\right)_{r=0} = -D_R k \phi_{B1}. \tag{3.56}$$

From Eqs. (3.55) and (3.56), we get

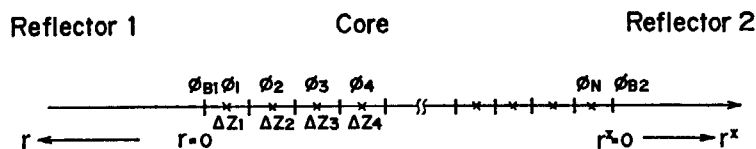


Fig. 3.5 Mesh distribution to calculate one-dimensional diffusion equation.

$$\phi_{B1} = A \cdot \phi_1, \quad (3.57)$$

$$\text{where } A = \frac{2D_1}{D_R k \Delta z_1 + 2D_1}, \quad (3.58)$$

The one-dimensional diffusion equation is expressed by the following difference equation for the first mesh point in the core region ;

$$D_1 \frac{\phi_1 - \phi_{B1}}{(\Delta z_1/2)} - D_1'(\phi_2 - \phi_1) + D_1 B^2 \phi_1 \Delta z_1 + \Sigma_{T1} \phi_1 \Delta z_1 = S_1 \Delta z_1, \quad (3.59)$$

$$\text{where } D_1' = \frac{2}{\frac{\Delta z_1}{D_1} + \frac{\Delta z_2}{D_2}}. \quad (3.60)$$

and the subscripts 1 and 2 refer to the first and second mesh points in the core region, respectively. Combining Eq. (3.57) with Eq. (3.59), we get

$$D_1 \frac{\phi_1 - A\phi_1}{(\Delta z_1/2)} - D_1'(\phi_2 - \phi_1) + D_1' B^2 \phi_1 \Delta z_1 + \Sigma_{T1} \phi_1 \Delta z_1 = S_1 \Delta z_1. \quad (3.61)$$

As  $A$  is a constant, Eq. (3.61) does not include any neutron flux terms of the reflector region, which allows us to solve the finite difference equations only in the core region.

The approach explained above is for the first energy group in the one-dimensional calculation, but the same approach is applicable to any other energy groups and also to the two-dimensional calculation.

### 3.3 Interfaces Between HYDRO-ACE and DIFUSION-ACE

As mentioned before, STEADY-ACE consists of the thermal-hydraulic part HYDRO-ACE and the three-dimensional neutron diffusion part DIFFUSION-ACE. The interfaces between these two parts are explained here.

The interface from the thermal-hydraulic part into the nuclear part is described first. The output of the thermal-hydraulic calculation is the block-wise void fraction within the channel box, while the input of the nuclear calculation is the block-wise neutron cross sections. SUBROUTINE CROSS serves as an interface by calculating the block-wise neutron cross sections from the block-wise void volume fraction within the channel box.

The neutron macroscopic cross sections are prepared as quadratic functions of the void fraction within the channel box.

$$\Sigma_x = (\Sigma_x^0) + (\Sigma_x^1) \cdot \alpha + (\Sigma_x^2) \cdot \alpha^2, \quad (3.62)$$

where  $\Sigma_x$  refers to the neutron cross sections, such as absorption cross section, slowing down cross section, diffusion coefficient and emission cross section (product of neutrons per fission and fission cross section).  $\alpha$  is a void fraction within the channel box.  $\Sigma_x^0$ ,  $\Sigma_x^1$  and  $\Sigma_x^2$  are fitting constants.

The fitting constants are prepared by the multi-group calculations for the lattice cells parametrically as a function of void fraction within the channel box. These parametric calculations produce two or three group cross sections homogenized over the lattice cells. It is assumed usually that the void fraction outside the channel box is zero. A quadratic fitting program processes these data into tables of the fitting constants. The tables of the fitting constants are prepared by the user and input into the program STEADY-ACE. Then, given the block-wise void fraction within the channel box from the thermal-hydraulic part HYDRO-ACE, the block-wise cross sections are calculated by Eq. (3.62).

The cross sections of the upper reflector region are also dependent on the void fraction. The table of the fitting constants for the upper reflector is also prepared by the user in the same manner as the table for the blocks. The void fractions at the outlet of the channels are used to determine the neutron cross sections for the upper reflector region.

As the void fractions in the lower reflector and side reflector regions are zero or close to zero, the void dependency of the neutron cross sections is not considered for these regions.

The interface from the nuclear part into the thermal-hydraulic part is described next. The output from the nuclear calculation is the normalized block-wise power distribution, where as the input to the thermal-hydraulic calculation is the block-wise thermal power distribution. Most of the heat generated in a block is transferred to the coolant within the channel box of the block, but some fraction of the heat is transferred to the coolant in the leakage flow by gamma-heating and heat transport through the channel boxes.

The heat transferred to the coolant within the channel box is obtained from the normalized power distribution :

$$q_{n,k} = Q \cdot (1 - \eta) \cdot \frac{P_{n,k}}{\sum_{n'} \sum_{k'} P_{n',k'}}, \quad (3.63)$$

where  $n$  : channel identification number

$k$  : axial position of the block

$q_{n,k}$  : heat transferred to the coolant within the channel box in the block ( $n, k$ ) [kcal/sec]

$Q$  : reactor thermal power [kcal/sec]

$\eta$  : heat fraction transferred to the coolant in the leakage flow path of the total heat generation

$P_{n,k}$  : normalized power of the block ( $n, k$ ).

The heat transferred to the coolant in the leakage flow path by gamma heating and heat transport through the channel boxes is calculated by

$$q_{L,k} = Q \cdot \eta \cdot \frac{\sum_{n'} P_{n',k'}}{\sum_{n'} \sum_{k'} P_{n',k'}}, \quad (3.64)$$

where  $L$  refers to the leakage flow path. The thermal power calculation by Eqs. (3.63) and (3.64) is performed in HYDRO-ACE.

The calculation starts from the initial power distribution guess specified by the user. From the power distribution the thermal-hydraulic subprogram HYDRO-ACE calculates the void fraction distribution. From the void fraction distribution, the subroutine CROSS calculates the neutron cross sections for the core and upper reflector regions. Given the cross sections, the nuclear subprogram DIFFUSION-ACE calculates the power distribution. The iterative calculations are performed until the consistency is obtained between the power and void fraction distributions. The convergence of the iteration is decided by comparing the power residuals with the convergence criterion specified by the user, where the power residual is defined as

$$(R_p)^n = \text{Max}_{l,k} \left| \frac{P^n - P^{n-1}}{P^n} \right|_{l,k}, \quad (3.65)$$

$n$  : number of iterations

$l$  : channel identification number

$k$  : axial block number

$P$  : normalized power of the block ( $l, k$ ).

The flow chart of the calculation is illustrated in Fig. 3.6.

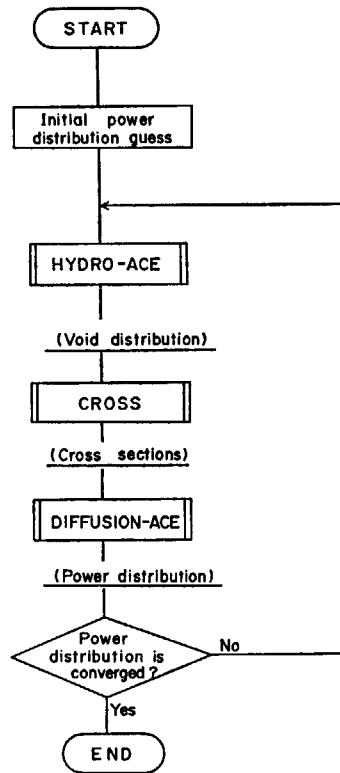


Fig. 3.6 General flow chart of STEADY-ACE.

## 4 Input Description

The input of STEADY-ACE consists of 70 classes of cards. Some classes of cards are not necessary, depending on the type of problems the user would like to solve. In general, (I3) formats are used for integer-type variables and (E10.0) or (F10.0) formats are used for real-type variables.

**Class 1** (18A4): Title card

col. 1~72 ITITLE: Problem name; the user can write any words for his own use.

**Class 2** (I3, 7X, 2E10.0): Convergence parameters for void-power iteration

col. 1~3 MAXCUP: Maximum number of void-power iterations.

col. 3~10 (blank)

col. 11~20 EPSCUP: Convergence criterion on power residual for void-power iteration, where power residual is defined by Eq. (3.65).

col. 21~30 WCUP: Relaxation factor for void-power iteration, where the new guess of power distribution for thermal-hydraulic calculation at the  $n$ -th iteration is calculated as

$$(P_{\text{guess}})_i^n = P_i^{n-1} \cdot \text{WCUP} + (1 - \text{WCUP}) \cdot P_i^{n-2}.$$

**Class 3** (7 I3): Options for thermal-hydraulic calculation

col. 1~3 KW1: (not used)

col. 4~6 KW2: (not used)

col. 7~9 KW3: (not used)

col. 10~12 KWDPFR: Option for two-phase friction loss multiplier

=0 Martinelli-Nelson correlation

=1 Sher's correction with Martinelli-Nelson correlation

=2 Armand's correlation

=3 Lottes-Finn's correlation

=4 The multiplier is specified by the user.  $\phi_{lt}$  in Eq. (3.7) is to be input.

=5 The multiplier is specified by the user.  $R_0$  in Eq. (3.9) is to be input.

col. 13~15 KWBALA: Option for calculation of core inlet enthalpy and feed-water enthalpy

=0 Feed-water enthalpy and core inlet enthalpy are calculated in the program by the heat balance equation. This option is available only for JPDR-II core calculation.

=1 Feed-water enthalpy is input. Core inlet enthalpy is calculated by the heat balance equation.

=2 Both feed-water enthalpy and core inlet enthalpy are input.

col. 16~18 KW6: (not used)

col. 19~21 KW7: (not used)

**Class 4** (7 I3): Option for pressure and heat balance calculations

col. 1~3 LPHYDR: Maximum number of iterations for pressure balance calculation to obtain the channel flow distribution.

col. 4~6 LP2: (not used)

col. 7~9 LPHIN: Maximum number of iterations for the heat balance calculation to obtain the core inlet enthalpy.

col. 10~12 LP4: (not used)

col. 13~15 LP5: (not used)



col. 16~18 LP6 : (not used)

col. 19~21 LP7 : (not used)

**Class 5** (7 E10.0) : Convergence criteria for pressure and heat balance calculations

col. 1~10 EPSHYD : Convergence criterion of pressure residual for the pressure balance calculation, where the residual is defined as

$$R_{\Delta P} = \text{Max}_l \left\{ \frac{(\Delta P)_l - (\Delta P)_{\text{ave.}}}{(\Delta P)_{\text{ave.}}} \right\},$$

$l$  : channel number

$(\Delta P)_l$  : pressure drop for channel  $l$

$(\Delta P)_{\text{ave.}}$  : pressure drop averaged over all channels

col. 11~20 EPS2 : (not used)

col. 21~30 EPSHIN : Convergence criterion for the heat balance calculation to determine the core inlet enthalpy.

col. 31~40 EPS4 : (not used)

col. 41~50 EPS5 : (not used)

col. 51~60 EPS6 : (not used)

col. 61~70 EPS7 : (not used)

**Class 6** (4 E10.0) : Elevation of channels (see Fig. 2.3)

col. 1~10 ZZIN : Elevation of the multi-channel zone inlet ;  $H_1$  in Fig. 2.3 [m].

col. 11~20 ZIN : Elevation of the bottom of the heated zone ;  $H_4$  [m]

col. 21~30 ZOUT : Elevation of the top of the heated zone ;  $H_5$  [m]

col. 31~40 ZZOUT : Elevation of the multi-channel zone exit ;  $H_6$  [m]

(Note) The vertical length of a block is calculated by

$$(DZ) = \frac{(ZOUT) - (ZIN)}{(KMAX)},$$

where (KMAX) is input in Class 7.

**Class 7** (A4, 2X, 4I3) : Core size (see Fig. 2.4)

col. 1~4 IZONE : Option for the calculation geometry

=(blank) Full core

=HALE 1/2 core

=QUAT 1/4 core.

col. 5~6 (blank)

col. 7~9 IMAX : Number of channels in the  $x$ -direction

col. 10~12 JMAX : Number of channels in the  $y$ -direction

col. 13~15 KMAX : Number of blocks in the  $z$ -direction

col. 16~18 NMAX : Number of channels in the core

**Class 8** (24 I3) : Core geometry for the nuclear calculation (see Fig. 2.4)

col. 1~ (NC(I, J), I=1, IMAX) : Channel type array for the nuclear calculation. The channel numbers are specified according to the X-coordinate I and Y-coordinate I in Fig. 2.4. The reflector zones of no channels are designated by 0.

(Note) (JMAX) cards of Class 8 are necessary.

**Class 9** (24 I3) : Core geometry for the thermal-hydraulic calculation (see Fig. 2.2)

col. 1~ (MG(N), N=1, NMAX+1) : Types of the thermal-hydraulic properties of channels. The last channel (NMAX+1) refers to the leakage flow channel. The thermal-hydraulic properties are in Classes 12, 13 and 14.

**Class 10** (3 E10.0) : Thermal-hydraulic constants

col. 1~10 PRESS : System absolute pressure [kg/cm<sup>2</sup>a].

col. 11~20 PHITT1 : Two phase multiplier correction factor.

col. 21~30 PHITT2 : Two phase multiplier correction factor.

(Note) PHITT1 and PHITT2 should be input only when KWDPFR in Class 3 is 4 or 5. The correction factors  $R_1$  in Eq. (3.7) and  $R_0$  in Eq. (3.9) are expressed by a quadratic equation of the steam quality  $x$  as

$$R_1 \text{ (or } R_0) = 1 + (\text{PHITT1}) \cdot x + (\text{PHITT2}) \cdot x^2.$$

**Class 11** (2 I3) : Channel types of the different thermal-hydraulic properties

col. 1~3 MGREAD : Number of channel types of the different thermal-hydraulic properties, corresponding to the maximum number in MG array in Class 9.

col. 4~6 KECCAL : Option for calculation of the expansion-contraction pressure loss factor (E/C factor).

=0 E/C factor is input.

=1 If the input specified E/C factors are positive, use the input value. If not, TABLE 3.1 is used to estimate the E/C factors.

=2 TABLE 3.1 is used to estimate the E/C factors.

**Class 12** (3 I3, 1X, A10, E10.0) : Thermal-hydraulic properties of channels (see Fig. 2.4)

col. 1~3 M : Channel type number.

col. 4~6 LMAX(M) : Number of sections in the channel type (M).

col. 7~9 NPSMAX : Number of spacers in the channel type (M).

col. 10 (blank)

col. 11~20 NAMEC(M) : Name referring to the channel type (M).

col. 21~30 HPERIM(M) : Heated peripheral area per unit length of the channel type (M) [m<sup>2</sup>/m]

**Class 13** (A4, 6X, 3 E10.0) : Thermal-hydraulic properties of the vertical sections in the channel type (M) (see Fig. 2.3)

col. 1~4 NAME(M, L) : Name referring to the section (L) in the channel type (M)

col. 5~10 (blank)

col. 11~20 ZZ(M, L) : Elevation of the inlet of the section (L) [m].

col. 21~30 A(M, L) : Flow area of the section (L) [m<sup>2</sup>].

col. 31~40 EC(M, L) : Expansion-contraction pressure loss factor at the inlet of the section (L).

(Note) (LMAX(M)+1) cards of Class 13 are necessary for each channel type.

**Class 14** (7 F 10.0) : Thermal-hydraulic properties of spacers in the channel type (M)

col. 1~ (ZSP(M, NSP), ECSP(M, NSP), NSP=1, NSPMAX)

ZSP : Elevation of spacers

ECSP : Spacer pressure loss coefficient.

(Note 1) Class 14 is input only when NSPMAX is positive. When NSPMAX ≥ 4, the input will continue to the subsequent cards.

(Note 2) (MGREAD) sets of Classes 12, 13 and 14 are necessary.

**Class 15** (A4) : Option for the initial power distribution for the thermal-hydraulic calculation

col. 1~4 METHOD : Option for the initial power distribution for the thermal-hydraulic calculation in the first power-void loop

=ALL : Initial power guess is input for all of the blocks.

=EACH : Channel power and axial power shape are specified by input in Classes 17 and 18 for each channel.

**Class 16** (7 E10.0) : Initial power distribution when METHOD=ALL

col. 1~ (S(N, K), K=1, KMAX) : Initial power guess of the block.

(Note) (NMAX) sets of Class 16 cards are necessary.

**Class 17** (3(A4, 6X, F10.0)) : Initial channel power and axial power shape when METHOD=EACH  
col. 1~4 NTYPE(N) : Option for axial power shape of the N-th channel

=CARD : Axial power distribution is specified by card input

=FLAT : Uniform distribution

=SINE : Sinusoidal distribution

=COMP : Bottom peaked distribution

=SAME : Power distribution calculated in the preceding case is used. This option cannot be used for the first case.

col. 5~10 (blank)

col. 11~20 SS(N) : Channel power of the N-th channel.

(Note) Each card includes input for 3 channels.

(NMAX/3+1) cards are necessary.

**Class 18** (7 F10.0) : Axial power distribution when METHOD=EACH and NTYPE(N)=CARD

col. 1~ (S(N, k), K=1, KMAX) : Axial power distribution.

(Note) Class 18 is repeated by the number of channels with NTYPE(N)=CARD.

**Class 19** (7 E10.0) : Core thermal parameters

col. 1~10 QTMW : Reactor thermal power [ $MW_{th}$ ].

col. 11~20 WTPH : Core inlet flow rate [ton/hr].

col. 21~30 WCLTPH : Flow rate of the clean-up line [ton/hr].

col. 31~40 ETA : Leakage flow fraction.

col. 41~50 XDC1 : Carry-under steam quality to down comer.

col. 51~60 BETA : Heat fraction transferred to the coolant in the leakage flow path of the total generated heat.

col. 61~70 NPCRL : Pump pressure [ $kg/m^2$ ].

**Class 20** (2 E10.0) : Inlet enthalpy when KWBALA  $\geq 1$

col. 1~10 HFEED : Feed-water enthalpy [kcal/kg]

col. 11~20 HIN : Core inlet enthalpy [kcal/kg]

**Class 21** (3 I3) : Option for neutron cross section input

col. 1~3 KKK : Option for input of the table of the fitting constants

=1 Fitting constants are the same for all the blocks

=2 Fitting constants are input for each block

=3 The blocks are categorized into the fuel types which have the same fitting constants.

col. 4~6 NGMAX : Number of energy groups. (NGMAX) should be either 2 or 3.

col. 7~9 NTMAX : Number of fuel types which have the same fitting constants. (NTMAX) should be specified when KKK=3.

(Note) When KKK=1 or 2, the fitting constants are input by Classes 22~28. When KKK=1, one set of Classes 22~28 is input. When KKK=2, (NMAX)\*(KMAX) sets of Classes 22~28 are input in sequence such as block 1 in channel 1, block 2 in channel 1, block 3 in channel 1, . . . ., block 1 in channel 2, . . . ., block (KMAX) in channel (NMAX). When KKK=3, the fitting constants are input by Classes 29~36.

**Class 22** (3 E10.0) : Fitting constants of diffusion coefficients of the fuel region when KKK=1 or 2

col. 1~10 D0 (N, K, NG) Fitting constants of the diffusion coefficient of the energy group

col. 11~20 D1 (N, K, NG) (NG) defined as

col. 21~30 D2 (N, K, NG)  $D^g = (D0)^g + (D1)^g \cdot \alpha + (D2)^g \cdot \alpha^2$ ,

where  $\alpha$  is the void fraction and  $g$  is the energy group.

(Note) (NGMAX) cards of Class 22 are necessary.

**Class 23** (3 E10.0) : Fitting constants of absorption cross sections of the fuel region when  $KKK=1$  or 2

col. 1~10 SVU0 (N, K, NG) Fitting constants of the emission cross section of the energy group

col. 11~20 SVU1 (N, K, NG) (NG) defined as

col. 21~30 SVU2 (N, K, NG)  $(\nu\Sigma_f)^g = (SVU0)^g + (SVU1)^g \cdot \alpha + (SVU2)^g \cdot \alpha^2$ .

The emission cross section is defined as the product of the number of neutrons per fission and the fission cross section.

(Note) (NGMAX) cards of Class 24 are necessary.

**Class 25** (3 E10.0) : Fitting constants of slowing-down cross sections of the fuel region when  $KKK=1$  or 2

col. 1~10 STR0 (N, K, NG) Fitting constants of the slowing-down cross section of the energy

col. 11~20 STR1 (N, K, NG) group (NG) defined as

col. 21~30 STR2 (N, K, NG)  $(\Sigma_r)^g = (STR0)^g + (STR1)^g \cdot \alpha + (STR2)^g \cdot \alpha^2$ .

(Note) (NGMAX) cards of Class 25 are necessary.

**Class 26** (3 E10.0) : Energy per fission when  $KKK=1$  or 2

col. 1~ (AKSF (N, K, NG),  $NG=1$ , NGMAX) : Released energy per fission for the energy group (NG).

**Class 27** (3 E10.0) : Number of neutrons per fission when  $KKK=1$  or 2

col. 1~ (ANU (N, K, NG),  $NG=1$ , NGMAX) : Emitted neutrons per fission for the energy group (NG).

**Class 28** (3 E10.0) : Initial leakage guess  $L_{xy}$  when  $KKK=1$  or 2

col. 1~ (ALXY (N, K, NG),  $NG=1$ , NGMAX) : Initial guess of the x-y direction leakage  $L_{xy}$  for the energy group (NG).

**Class 29** (24 I3) : Fuel type when  $KKK=3$

col. 1~ (NTYPE (N, K),  $K=1$ , KMAX) : Fuel type number of the block (n, k). A fuel group has the same fitting constants.

(Note) (NMAX) cards of Class 29 are necessary.

**Class 30** (3 E10.0) : Fitting constants of diffusion coefficients of the fuel region when  $KKK=3$

col. 1~10 DTP0 (NT, NG) Fitting constants of the diffusion coefficient of the energy group

col. 11~20 DTP1 (NT, NG) (NG) for the fuel type (NT).

col. 21~30 DTP2 (NT, NG)

(Note) (NGMAX) cards of Class 30 are necessary.

**Class 31** (3 E10.0) : Fitting constants of absorption cross sections of the fuel region when  $KKK=3$

col. 1~10 SSATP0 (NT, NG) Fitting constants of the absorption cross section of the energy

col. 11~20 SSATP1 (NT, NG) group (NG) for the fuel type (NT).

col. 21~30 SSATP2 (NT, NG)

(Note) (NGMAX) cards of Class 31 are necessary.

**Class 32** (3 E10.0) : Fitting constants of the emission cross sections of the fuel region when  $KKK=3$

col. 1~10 SVUTP0 (NT, NG) Fitting constants of the emission cross sections of the energy

col. 11~20 SVUTP1 (NT, NG) group (NG) for the fuel type (NT).

col. 21~30 SVUTP2 (NT, NG)

(Note) (NGMAX) cards of Class 32 are necessary.

**Class 33** (3 E10.0) : Fitting constants of the slowing-down cross sections of the fuel region when  $KKK=3$

col. 1~10 STRTP0 (NT, NG) Fitting constants of the slowing-down cross sections of the energy

col. 11~20 STRTP1 (NT, NG) group (NG) for the fuel type (NT).

col. 21~30 STRTP2 (NT, NG)

(Note) (NGMAX) cards of Class 33 are necessary.

**Class 34** (3 E10.0) : Energy per fission when KKK=3

col. 1~ (AKSFTP (NT, NG), NG=1, NGMAX) : Released energy per fission for the energy group (NG)

**Class 35** (3 E10.0) : Number of neutrons per fission when KKK=3

col. 1~ (ANUTR (NT, NG), NG=1, NGMAX) : Emitted neutrons per fission for the energy group (NG)

**Class 36** (3 E10.0) : Initial leakage guess  $L_{xy}$  when KKK=3

col. 1~ (ALXYTP (NT, NG), NG=1, NGMAX) : Initial guess of the x-y direction leakage  $L_{xy}$  for the energy group (NG).

**Class 37** (3 E10.0) : Diffusion coefficients of the upper reflector region

col. 1~10 SSAT0 (NG) Fitting constants of the absorption cross section of the energy group

col. 11~20 SSAT1 (NG) (NG) for the upper reflector region.

col. 21~30 SSAT2 (NG)

(Note) (NGMAX) cards of Class 38 are necessary.

**Class 39** (3 E10.0) : Slowing-down cross sections of the upper reflector region.

col. 1~10 STRT0 (NG) Fitting constants of the slowing-down cross section of the energy group

col. 11~20 STRT1 (NG) (NG) for the upper reflector region.

col. 21~30 STRT2 (NG)

(Note) (NGMAX) cards of Class 39 are necessary.

**Class 40** (3 E10.0) : Buckling of the upper reflector region

col. 1~10 BUKT0 (NG) Fitting constants of the buckling  $B^2$  of the energy group (NG) for col. 11~20 BUKT1 (NG) the upper reflector region.

col. 21~30 BUKT2 (NG)

(Note) (NGMAX) cards of Class 40 are necessary.

**Class 41** (4 E10.0) : Cross sections of the lower reflector region

col. 1~10 DB (NG) : Diffusion coefficient of the energy group (NG) for the lower reflector region.

col. 11~20 SSAB (NG) : Absorption cross section of the energy group (NG) for the lower reflector region.

col. 21~30 STRB (NG) : Slowing-down cross section of the energy group (NG) for the lower reflector region.

col. 31~40 BUKB (NG) : Buckling of the energy group (NG) for the lower reflector region.

(Note) (NGMAX) cards of Class 41 are necessary.

**Class 42** (4 E10.0) : Cross sections of the side reflector region

col. 1~10 DR (NG) : Diffusion coefficient of the energy group (NG) for the side reflector region.

col. 11~20 SSAR (NG) : Absorption cross section of the energy group (NG) for the side reflector region.

col. 21~30 STRR (NG) : Slowing down cross section of the energy group (NG) for the side reflector region.

col. 31~40 BUKR (NG) : Buckling of the energy group (NG) for the side reflector region.

(Note) (NGMAX) cards of Class 42 are necessary.

**Class 43** (5 I3) : Subdivision for diffusion equation calculation

col. 1~3 ISECT : Number of subdivisions in a block in the x-direction.

col. 4~6 JSECT : Number of subdivisions in a block in the y-direction.

col. 7~9 KSECT : Number of subdivisions in a block in the z-direction.

col. 10~12 NRMIV : Number of mesh points in the side reflector region in the x or y direction.

col. 13~15 NZR: Number of mesh points in the upper or lower reflector region in the  $z$  direction

**Class 44** (6 I3): Options for diffusion equation calculation

col. 1~3 NCROD: Number of control rods ( $\leq 16$ ).

col. 4~6 INMAX: Number of in-core-monitors ( $\leq 30$ ).

col. 7~9 NSKO: Number of the subdivisions for smaller mesh width. In the  $z$ -directional one-dimension diffusion calculation, some of the subdivisions are further divided into 3 equal meshes in order to calculate the local effect of the control rods on the power distribution (see Class 48).

col. 10~12 MNZ: In the case of analytical boundary condition, the neutron fluxes in the lower and upper reflector regions are edited at (MNZ) points ( $\leq 30$ ) (see Class 49).

col. 13~15 IGS: Option for initial guess of the neutron source distribution

=0 Initial guess of the horizontal leakage  $L_{xy}$  is input. The source distribution is calculated from  $L_{xy}$ .

=1 Initial guess of the neutron source distribution is input (see Classes 66, 67 and 68).

col. 16~18 IPUNCH: Option for punch output

=0 No punch output

=1 The source distribution is punched so that it can be used as an initial guess for the next case (see Classes 66, 67 and 68).

**Class 45** (5 E10.0): Geometry for the diffusion equation calculation

col. 1~10 DX: Block width in the  $x$ -direction [cm].

col. 11~20 DY: Block width in the  $y$ -direction [cm].

col. 21~30 RFWID: Width of the side reflector region in the two-dimensional calculation [cm].

col. 31~40 CRWID: Width of the control rod [cm].

col. 41~50 REFZ: Length of the upper and lower reflector regions in the one-dimensional calculation [cm].

**Class 46** (8 I3, 6X, E10.0): Control rod position. This class 46 is necessary only when NCROD > 0

col. 1~3 L: Control rod identification number.

col. 4~6 ICR (L): Position of the control rod (L) in the  $x$ -direction. Use X-coordinate II in **Fig. 2.4**.

col. 7~9 JCR (L): Position of the control rod (L) in the  $y$ -direction. Use Y-coordinate II in **Fig. 2.4**.

col. 10~12 (NEIBCR (N, L), M=1, 4): Identification numbers of the fuel assemblies neighbouring the control rod (L). The sequence of the four assemblies can be selected arbitrarily.

col. 13~15

col. 16~18

col. 19~21

col. 22~24 KCR (L): Block number of the tip position of the control rod (L).

col. 25~30 (blank)

col. 31~40 ZCR (L): Elevation of the tip of the control rod (L) from the bottom of the core [cm].

(Note) (NCROD) cards of Class 46 are necessary.

**Class 47** (3 I3): Position of the in-core-monitors. Class 47 is necessary only when (INMMAX > 0 (see Class 44).

col. 1~3 K: Identification number of the in-core-monitor.

col. 4~6 IIN (K): Position of the in-core-monitor (K) in the  $x$ -direction. Use X-coordinate II in **Fig. 2.4**.

col. 7~9 JIN (K): Position of the in-core-monitor (K) in the  $y$ -direction. Use Y-coordinate II in **Fig. 2.4**.

(Note) (INMMAX) cards of Class 47 are necessary.

**Class 48** (24 I3): Position of fine divisions. Class 48 is necessary only when  $NSKO > 0$  (see Class 44).

col. 1~ (NSPNO (I), I=1, NSKO): Identification number of  $z$ -directional mesh to be further divided (see Fig. 2.5 for the mesh identification number).

**Class 49** (E10.0): Neutron flux edit for the upper and lower reflector regions. Class 49 is necessary only when  $(MNZ) > 0$

col. 1~10 DLZ: Interval of the points in the upper and lower reflector regions at which the neutron fluxes are calculated and edited [cm].

**Class 50** (6 I3): Boundary conditions (see Figs. 2.4 and 2.5)

col. 1~3 KLB: Option for the bottom boundary condition ( $z$ -direction).

col. 4~6 KRT: Option for the top boundary condition ( $z$ -direction).

col. 7~9 KL: Option for the left boundary condition ( $x$ -direction).

col. 10~12 KR: Option for the right boundary condition ( $x$ -direction).

col. 13~15 KB: Option for the back-side boundary condition ( $y$ -direction).

col. 16~18 KT: Option for the front-side boundary condition ( $y$ -direction).

4 Options can be selected for each of the boundary conditions.

=0 Zero flux:  $\phi = 0$

=1 Zero derivative:

$$\left(\frac{d\phi}{dr}\right) = 0$$

=2 Logarithmic derivative:

$$\left(\frac{d\phi}{dr}\right) = -\frac{\phi}{\gamma},$$

Where the derivative  $\gamma$  is specified by the user in classes 51~56.

=3 Neutron flux distribution outside the boundary is calculated analytically.

**Class 51** (3 E10.0): Class 51 is necessary only when  $KLB = 2$

col. 1~ (C1 (NG), NG=1, NGMAX): Logarithmic derivative at the bottom boundary for the energy group (NG).

**Class 52** (3 E10.0): Class 52 is necessary only when  $KRT = 2$

col. 1~ (C2 (NG), NG=1, NGMAX): Logarithmic derivative at the top boundary for the energy group (NG).

**Class 53** (3 E10.0): Class 53 is necessary only when  $KL = 2$

col. 1~ (C3 (NG), NG=1, NGMAX): Logarithmic derivative at the left boundary for the energy group (NG).

**Class 54** (3 E10.0): Class 54 is necessary only when  $KR = 2$

col. 1~ (C4 (NG), NG=1, NGMAX): Logarithmic derivative at the right boundary for the energy group (NG).

**Class 55** (3 E10.0): Class 55 is necessary only when  $KB = 2$

col. 1~ (C5 (NG), NG=1, NGMAX): Logarithmic derivative at the back-side boundary for the energy group (NG).

**Class 56** (3 E10.0): Class 56 is necessary only when  $KT = 2$

col. 1~ (C6 (NG), NG=1, NGMAX): Logarithmic derivative at the front-side boundary for the energy group (NG).

**Class 57** (3 E10.0): Fission spectrum

col. 1~ (YK (NG), NG=1, NGMAX): Energy spectrum of fission neutrons.

**Class 58** (3 I3): Convergence parameters of the diffusion calculation to derive the initial value of

the 3-D source distribution.

col. 1~3 ITIN1 : Maximum number of the inner iterations of the 2-D diffusion calculation.

col. 4~6 IPMAX1 : Maximum number of the source iterations of the 2-D diffusion calculation  
 =0 SLOR (Successive Line Over Relaxation) method is applied both to the  
 $x$ - and  $y$ -directions  
 =1 SLOR method is applied to the  $x$ -direction.

**Class 59** (4 E10.0) : Convergence parameters of the diffusion calculation to obtain the initial value of the 3-D source distribution

col. 1~10 EPSI (1) : Convergence criterion on the eigenvalue of the 1-D calculation.

col. 11~20 EPSI (2) : Convergence criterion on the source distribution of the 1-D calculation.

col. 21~30 EPS2 : Convergence criterion in the inner iteration of the 2-D calculation.

col. 31~40 EPS1 : Convergence criterion in the source iteration of the 2-D calculation.

**Class 60** (2 E10.0) : Acceleration parameters in the diffusion calculation to obtain the initial value of the 3-D source distribution

col. 1~10 THETA : Acceleration factor of the source iteration of the 1-D calculation.

col. 11~20 W : Acceleration factor of the source iteration of the 2-D calculation.

**Class 61** (4 I3) : Convergence parameters of the 3-D diffusion equation calculation

col. 1~3 IP3MAX : Maximum number of the outer iterations of the 3-D calculation.

col. 4~6 ITMAX : Maximum number of the inner iterations of the 3-D calculation.

col. 7~9 ITR1 : Number of the outer iteration cycles to determine the convergence criteria for  
 col. 10~12 ITR2 the inner iterations of the 3-D calculation.

**Class 62** (3 E10.0) : Convergence parameters of the 3-D diffusion calculation

col. 1~10 EPI (1) : Temporary convergence criterion in the inner iteration of the 3-D calculation. This criterion is applied to the outer iteration cycles of less than (ITR1) in the first void-power iteration cycle.

col. 11~20 EPI (2) : Temporary convergence criterion in the inner iteration of the 3-D calculation. This criterion is applied to the outer iteration cycles of greater than (ITR1+1) and less than (ITR2) in the first void-power iteration cycle.

col. 21~30 EPI (3) : Final convergence criterion of the inner iteration of the 3-D calculation.

**Class 63** (2 I3) : Convergence parameters of the 3-D diffusion calculation

col. 1~3 IDF1 : Number of the power-void iteration cycles to determine the convergence criteria

col. 4~6 IDF2 : for the outer iterations of the 3-D calculation.

**Class 64** (3 E10.0) : Convergence parameters of the 3-D diffusion calculation

col. 1~10 CRT31 : Temporary convergence criterion in the outer iteration of the 3-D calculation. This criterion is applied to the power-void iteration cycles of less than (IDF1).

col. 11~20 CRT32 : Temporary convergence criterion in the outer iteration of the 3-D calculation. This criterion is applied to the power-void iteration cycles of greater than (IDF1+1) and less than (IDF2).

col. 21~30 CRT33 : Final convergence criterion in the outer iteration of the 3-D calculation.

**Class 65** (3 E10.0) : Acceleration parameters in the 3-D calculation

col. 1~10 WXY : Acceleration factor of  $L_{xy}$  in the 3-D inner iterations.

col. 11~20 WZS : Acceleration factor of  $L_z$  in the 3-D inner iterations.

col. 21~30 WS : Acceleration factor of the 3-D outer iterations.

**Class 66** (3 I3) : Number of the mesh points when IGS=0

col. 1~3 NAMAX : Number of the mesh points in the  $z$ -direction.

col. 4~6 IIMAX : Number of the mesh points in the  $x$ -direction.



col. 7~9 JJMAX : Number of the mesh points in the  $y$ -direction. .

(Note) Class 66 is necessary only when  $IGS \neq 0$ . Classes 66 through 68 uses punched cards from the previous calculation.

**Class 67** (7 E10.0) : Initial guess of the source distribution when  $IGS \neq 0$

col. 1~ (A (N), N=1, NAMAX) : Initial guess of the source distribution in the 1-D calculation.

(Note) Class 67 is required only when  $IGS \neq 0$ . (NMAX) sets of Class 67 are necessary.

**Class 68** (7 E10.0) : Initial guess of the source distribution when  $IGS \neq 0$

col. 1~ (A (N), N=1, KKKMAX) : Initial guess of the source distribution in the 2-D calculation  
(KKKMAX=IIMAX\*JJMAX).

(Note) Class 68 is required only when  $IGS=0$ . (KMAX) sets of Class 68 are necessary.

**Class 69** (7 E10.0) : Nuclear cross sections of the control rod when  $NCROD \neq 0$

col. 1~10 GBASE (NG) : Logarithmic derivative of the energy group (NG) for the control rod.

col. 11~20 GDD (NG) : Diffusion coefficient of the energy group (NG) for the control rod.

col. 21~30 GSR (NG) : Slowing-down cross section of the energy group (NG) for the control rod.

col. 31~40 GSA (NG) : Absorption cross section of the energy group (NG) for the control rod.

col. 41~50 GCR (NG) : Initial guess of the neutron leakage of the energy group (NG) into the control rod.

(Note) Classes 69 and 70 are required only when  $NCROD \neq 0$ . (NGMAX) sets of Class 69 are necessary.

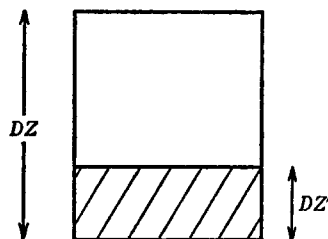
**Class 70** (E10.0) : Correction parameter of the control rod nuclear constants when  $NCROD \neq 0$

col. 1~10 WHT : Correction factor of the logarithmic derivative for the tip of the control rod :

$$\frac{\partial \phi}{\partial r} = -\frac{\phi}{\gamma}$$

GBASE (NG) in Class 69 is the logarithmic derivative ( $-\gamma$ ) in the above equation. When the tip of the control rod is in the middle of a block, the logarithmic derivative for the block is given by

$$-\gamma' = \text{GBASE (NG)} * \frac{DZ}{DZ'} * \text{WHT}$$



## 5 Major Output

STEADY-ACE gives print-out output and punched card output.

### 5.1 Print-out

STEADY-ACE gives the following output in addition to the print-out of the input data.

- (1) Eigenvalue.
- (2) Block-wise power distribution.
- (3) Block-wise group-wise neutron flux distribution.
- (4) Block-wise group-wise leakage distribution.
- (5) Assembly power.
- (6) Assembly flow.
- (7) Pressure drop and its components.
- (8) Core average void fraction.
- (9) Block-wise distribution of heat flux, void fraction, quality, moderator density and CHF (critical heat flux ratio).
- (11) Gross peaking and MCHFR (minimum critical heat flux ratio).
- (12) Neutron flux distribution in the reflector region.
- (13) Thermal neutron flux at the in-core-monitor.

### 5.2 Punched Cards

STEADY-ACE has an option to give punched card output. Punched cards can be utilized as input cards in the subsequent calculations. Use of the punched cards reduces the computation time in the subsequent calculations significantly.

- (1) Mesh-wise source distribution: The output cards will be the input data of Classes 66, 67 and 68 in the subsequent calculations as an initial guess of the source distribution.
- (2) Block-wise horizontal leakage distribution  $L_{xy}$ : The output cards will be the input data of Class 28 in the subsequent calculations as an initial guess of the horizontal leakage distribution.

## 6 Numerical Examples

### 6.1 Sample Input and Output of STEADY-ACE

The JPDR-II core was analyzed to demonstrate the applicability of STEADY-ACE. A quarter symmetry was assumed to simplify the calculation. The JPDR-II core parameters and the geometry were described already in **Chapter 2**. The nuclear cross sections of the JPDR-II fuel assemblies were derived from the JPDR-II core design report<sup>7)</sup>. The input data listings and output results for the example case are attached in the Appendices **A** and **B**, respectively. The computation time for the example case was 7 minutes for CPU time or 28 minutes for CORE time on the machine FACOM-230-75. The convergence history of power-void iteration is shown in **TABLE 6.1** from which it is seen that the iterative scheme is converged smoothly.

**TABLE 6.1** Convergence history of power-void iteration

No. of power-void iteration	No. of outer iteration	Eigenvalue	Relative error of power-void iteration
1	1	1.00323	—
1	2	1.00550	—
1	3	1.00409	—
1	4	1.00364	—
1	5	1.00328	—
1	6	1.00303	—
1	7	1.00326	—
1	8	1.00317	—
2	2	1.00780	—
2	3	1.00844	—
2	4	1.00844	—
2	5	1.00842	—
3	2	1.00868	0.020602
4	2	1.00883	—
4	3	1.00894	0.022520
5	2	1.00900	0.006153
6	2	1.00899	0.002230
7	2	1.00899	0.000811

### 6.2 Power Distribution in JPDR-II Core

The power distribution in JPDR-II core was estimated by measuring decay  $\gamma$ -rays of Ti-Cu wires in in-core monitors. A comparison of the power distribution obtained by measurement with the calculated result by STEADY-ACE is shown in **Figs. 6.1** and **6.2**. **Figure 6.1** shows the axial power distributions in channels located at (16, 5), (17, 5) and (18, 5) in **Fig. 2.1**. The channels (16, 5) and (17, 5) are close to a control rod which is inserted into NO. 8 block from bottom. This figure shows the calculated power distributions near the control rod are flatter than measured ones. This is caused by an over-estimation of the neutron leakage to the control channel from neighbouring channels. **Figure 6.2** shows the heat production rate in JPDR-II core. The heat rate in channels near the reflector is over estimated. The large errors, appear in channels near reflector or control rods, but the value is less than 10% at the region of the maximum power peaking.

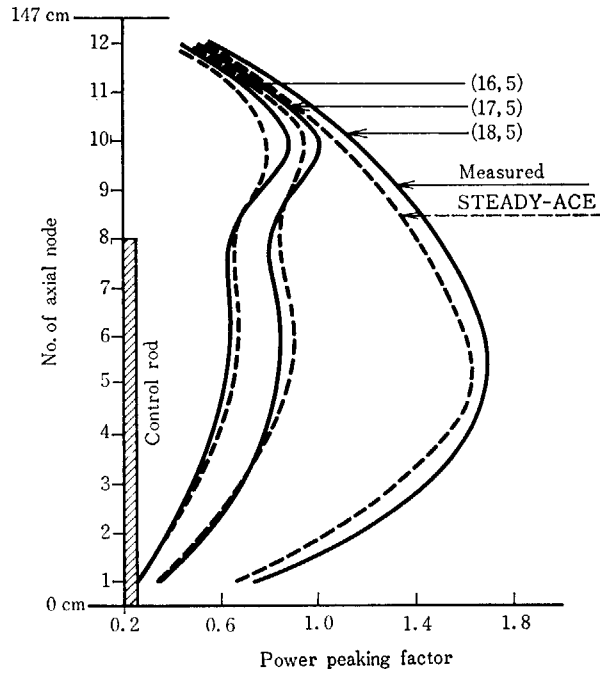


Fig. 6.1 Axial power distribution normalized to core average of unity

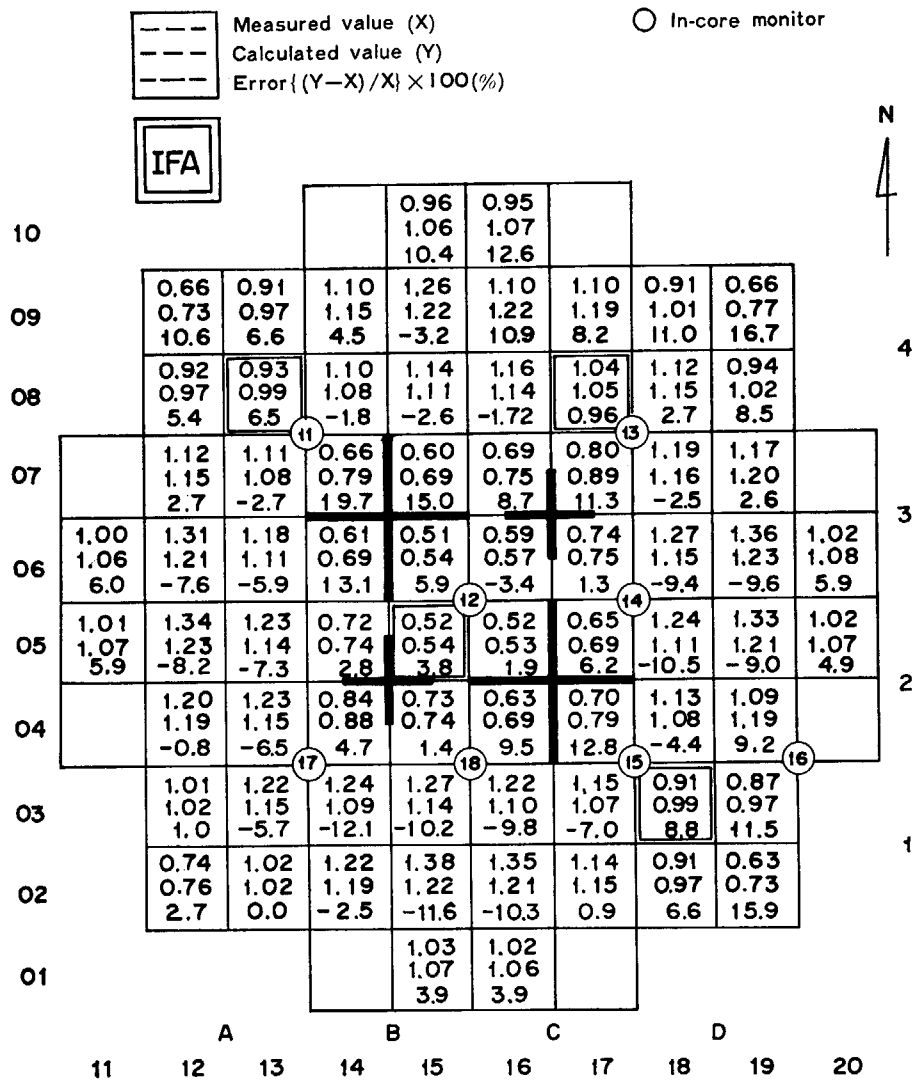


Fig. 6.2 Heat production rate in JPDR-II core

### 6.3 Coolant Flow Distribution in JPDR-II Core

Four instrumented fuel assemblies (IFA) were loaded in JPDR-II core and the coolant flow rate through IFA's were measured by a turbine flow meter attached to the inlet and the outlet of IFA's as shown in Fig. 6.3. Calculated coolant flow rates through IFA's were compared with the measured data and the results are given in TABLES 6.2 and 6.3. TABLE 6.2 shows that the calculated results are in agreement with measured ones within a few percent error. In TABLE 6.3 are shown relations between the nomalized heat production rate and the coolant flow rate. The more heat is produced in a channel, the less coolant flows through the channel near the rated flow rate (100% flow) but the more coolant flows at less than 80% flow rate. The

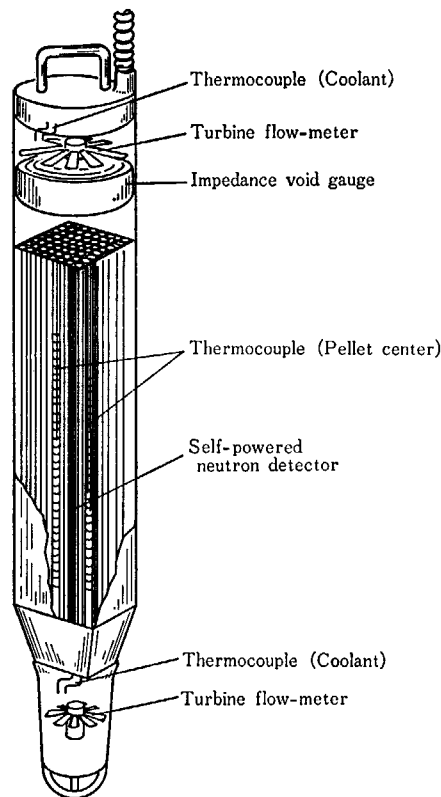


Fig. 6.3 JPDR-II instrumented fuel assembly

TABLE 6.2 Comparison of flow rate in IFA channels between calculation and measurement

Nominal flow rate		%	100	80	60	40
IFA HYDRO-ACE Error	# 4	kg/sec	6.50	5.10	4.04	2.80
	(15, 6)	kg/sec	6.28	4.97	3.72	2.72
		%	-3.38	-2.55	-7.92	-2.86
IFA HYDRO-ACE Error	# 5	kg/sec	6.39	5.29	4.31	3.44
	(13, 3)	kg/sec	6.51	5.34	4.26	3.40
		%	+1.88	+0.95	-1.16	-1.16
IFA HYDRO-ACE Error	# 6	kg/sec	6.65	5.56	4.27	3.59
	(18, 8)	kg/sec	6.52	5.35	4.27	3.42
		%	-1.95	-3.78	-0.0	-4.74
IFA HYDRO-ACE Error	# 7	kg/sec	6.50	5.56	4.50	3.78
	(17, 3)	kg/sec	6.55	5.41	4.35	3.53
		%	+0.77	-2.70	-3.33	-6.61

TABLE 6.3 Dependency of coolant flow rate on heat production

	Location of assembly	Normalized heat production rate in assembly	Coolant flow rate (kg/sec)			
			Nominal value (%)			
			100	80	60	40
Calculated by STEADY-ACE	(12, 6)	1.349	10.90	8.79	6.83	5.32
	(11, 5)	1.003	11.09	8.78	6.61	4.92
	(15, 5)	0.508	11.22	8.42	5.84	3.73
Measured	IFA #4	0.557	6.50	5.10	4.04	2.80
	IFA #5	0.912	6.39	5.29	4.31	3.44

above coolant flow characteristics in JPDR-II core are obtained both by measurement and by calculation. This shows again that STEADY-ACE is applicable to analyse efficiently the core performance of a BWR.

## 7 Conclusion

STEADY-ACE provides a very useful tool to make an accurate prediction of the BWR core performance in a reasonably short computation time. The applicability of the program are very wide. For example, it is useful for the detailed analysis of the start-up tests and the calibration of the simplified program such as FLARE<sup>1)</sup>.

The limitations of the computer program are as follows :

1. The program is applicable only to BWR core analyses, as the cross flow through the channel boxes are not included in the thermal-hydraulic subprogram HYDRO-ACE.
2. The exposure dependency of the unclear cross sections is not included in the program. Further efforts are required to make the program applicable to the control rod search for the exposed core and other core management analyses.

## Acknowledgment

DIFFUSION-ACE, which is a major component of STEADY-ACE, was programmed with the assistance of Mr. Kazuo Shibuya (Fujitsu Co. Inc.). The authors express their appreciation for his great efforts. Thanks also due to S. Matsuura of JAERI for his valuable discussion and his critical reading of this manuscript.

## Reference

- 1) Delp D. L., Fischer P. L., Harri-Man J. M. : "FLARE, A Three-Dimensional Boiling Water Reactor Simulator", GEAP-4598 (1964).
- 2) Moriguchi K. et. al. : "JP-Hydro, A Computer Program for Thermal-Hydraulic Analysis of a Natural Circulation Boiling Water Reactor", JAERI 1108 (1966) (in Japanese).
- 3) Abe K., Naito Y. : "Computer Code HYDRO-ACE for Analyzing Thermo-Hydraulic Phenomena in a BWR Core", JAERI-M 8442 (1979) (in Japanese)
- 4) Naito Y., Maekawa M., Shibuya K. : "A Three-Dimensional Neutron Diffusion Calculation Code, DIFFUSION-ACE", JAERI-1262 (1979).
- 5) Naito Y., Maekawa M., Shibuya K. : "A Leakage Iteration Method for Solving the Three-Dimensional Neutron Diffusion Equation", *Nucl. Sci. Eng.*, **58**, 182 (1975).
- 6) Maurer G. W. : "A Method of Predicting Steady State Vapor Fractions in Reactor Coolant Channels", WAPD-BT-19 (1960).
- 7) JPDR-II Project Core Design Group : "JPDR-II Core Design Report", JAERI-memo 4346 (published in 1971) (in Japanese).

Appendix A : STEADY-ACE Sample Input

```

                JPDR      A QUARTER CORE
25             0.01      1.5

10 10 10 10 10 10 1
0.01      0.01      0.01      0.01      0.01      0.01
2.078     2.323     3.790     3.9415
QUAT      5 8 11
          0 11
          0 10 9 7 5
          0 9 8 6 4
          0 7 6 3 2
          11 5 4 2 1
          1 1 1 1 1 1 1 1 1 1 2
          62.5
          2 0
          1 5 2 JP-2 7*7 1.883
SUPP      2.078     0.005027 0.08      0.4038
EXPA      2.128     0.0006362 0.09      0.
TIE       2.211     0.008339 0.0142    0.75
FUEL      2.236     0.008339 0.0142    0.
TIE       3.894     0.008339 0.0142    0.28
DUMMY     3.9415
          2.768     0.526     3.308     0.526
          2 3 0 LEAKAGE 0.
SUP1      2.078     0.00896 0.038     0.6742
SUP2      2.109     0.04864 0.028     0.2569
FUEL      2.128     0.2485 0.0148    0.6468
DUMMY     3.9415
          0.4913
EACH
SINE      1.      SINE      1.      SINE      1.
SINE      1.      SINE      1.      SINE      1.
SINE      1.      SINE      1.      SINE      1.
SINE      1.      SINE      1.      SINE      1.
          90.      3260.      3.4      0.1      0.002      0.018      0.
          3 3 1
          1 1 1 1 1 1 1 1 1 1 1 1
          1 1 1 1 1 1 1 1 1 1 1 1
          1 1 1 1 1 1 1 1 1 1 1 1
          1 1 1 1 1 1 1 1 1 1 1 1
          1 1 1 1 1 1 1 1 1 1 1 1
          1 1 1 1 1 1 1 1 1 1 1 1
          1 1 1 1 1 1 1 1 1 1 1 1
          1 1 1 1 1 1 1 1 1 1 1 1
          1 1 1 1 1 1 1 1 1 1 1 1
          1 1 1 1 1 1 1 1 1 1 1 1
          1 1 1 1 1 1 1 1 1 1 1 1
          1 1 1 1 1 1 1 1 1 1 1 1
          1.6903     0.43880 0.31036
          0.80625     0.30666 0.27090
          0.41354     0.16192 0.34548
          .0028169 -0.27275E-3-.31258E-4
          .016610     .63046E-3 .75624E-2
          0.62154     -.78250E-2-.77068E-2
          .33217E-2-.28149E-3-.21250E-3
          .94623E-2 .46148E-3 .30625E-2
          .87355E-1-.75121E-2-.13957E-1
          .39588E-1-.23115E-1-.77498E-3
          .63019E-1-.45938E-1-.29378E-2
          0.
          3.111E-11 3.111E-11 3.111E-11
          2.645     2.43     2.442
          3.619E-03 1.726E-03 8.840E-04
          2.66193     1.33137 0.992551
          1.04664     0.588856 0.542857

          0.390606 0.238981 0.266002
          .30503E-3-.24231E-3 .42850E-5
          .79612E-3-.31560E-3 .25986E-8
          .13988E-1-.48697E-2-.48570E-3
          .35692E-1-.24104E-1-.99951E-4
          .70755E-1-.50182E-1-.14303E-4

          .1020 E-2
          .1020 E-2
          .1020 E-2
          2.66193     0.0003050 0.0356918 .10200E-2
          1.04664     0.0027657 0.0707551 .10200E-2
          0.390606 0.0391508 .10200E-2
          2.2459     0.000565 0.054836 .38210E-3
          0.7790     0.000719 0.114673 .38210E-3
          0.2501     0.010986 .38210E-3
          2 2 3 1 0

          13.66     13.66     0.1      0.      0.
          3 3 3 1 3 1
          1.
          50 50 1
          0.01      0.01      0.01      0.01
          0.8      1.4
          30100 3 5
          0.005     0.003     0.001
          3 5
          0.005     0.003     0.001
          0.0      0.0      1.5
    
```



### Appendix B: STEADY-ACE Sample Output

\*\*\* VERTICAL PLANE FIGURE \*\*\*

```

MULTI-CHANNEL ZONE
OUTLET HEIGHT          = 3.9415  -----

HEATED ZONE
OUTLET HEIGHT = ZN( 9) = 3.7900  -----   Z( 9) = 3.7900
                                           Z( 8) = 3.6983
                                           Z( 7) = 3.5149
                                           Z( 6) = 3.3316
                                           Z( 5) = 3.1482
                                           Z( 4) = 2.9648
                                           Z( 3) = 2.7814
                                           Z( 2) = 2.5981
                                           Z( 1) = 2.4147
                                           -----
                                           ZN( 8) = 3.6066  -----
                                           ZN( 7) = 3.4233  -----
                                           ZN( 6) = 3.2399  -----
                                           ZN( 5) = 3.0565  -----
                                           ZN( 4) = 2.8731  -----
                                           ZN( 3) = 2.6898  -----
                                           ZN( 2) = 2.5064  -----
HEATED ZONE
INLET HEIGHT   = ZN( 1) = 2.3230  -----

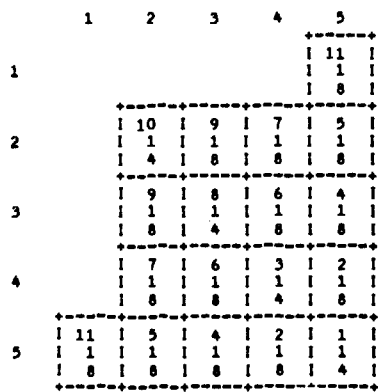
MULTI-CHANNEL ZONE
INLET HEIGHT          = 2.0780  -----

ZN(KK) = NODE POINT HEIGHT          Z(K) = BLOCK MIDDLE
                                         POINT HEIGHT

KMAX1 = 9                            KMAX = 8

LENGTH OF A REGION (DZ) = 0.1834
    
```

\*\*\* ARRANGEMENT OF ASSEMBLIES \*\*\*  
QUAT REGION OF THE CORE



LEAKAGE  
12  
2  
1

NOTE  
N | CONDITIONED NUMBER  
M6 | GEOMETRICAL TYPE NUMBER  
NO | OCCUPIED NUMBER

\* NCHANL = SIGMA(NO(N)) = 72 N=1      \* NCHAN1 = SIGMA(NO(N)) = 73 N=1      \* NBLOCK = KMAX\*NCHANL = 576

## \*\*\* PROPERTIES OF WATER AND STEAM \*\*\*

ABSOLUTE PRESSURE ..... 62.5 KG/CM\*\*2  
 ( 889.0 PSIA )  
 ENTHALPY OF SATURATED WATER ..... 291.6 KCAL/KG  
 ENTHALPY OF SATURATED STEAM ..... 664.9 KCAL/KG  
 SATURATION TEMPERATURE ..... 276.9 DEG-C  
 DENSITY OF SATURATED WATER ..... 755.9 KG/M\*\*3  
 DENSITY OF SATURATED STEAM ..... 31.6 KG/M\*\*3  
 DYNAMIC VISCOSITY OF SATURATED WATER ..... 0.98962E-05 KG·SEC/M\*\*2  
 KINEMATIC VISCOSITY OF SATURATED WATER .... 0.12839E-06 M\*\*2/SEC  
 DYNAMIC VISCOSITY OF SATURATED STEAM ..... 0.18972E-05 KG·SEC/M\*\*2  
 KINEMATIC VISCOSITY OF SATURATED STEAM .... 0.58970E-06 M\*\*2/SEC  
 THERMAL CONDUCTIVITY OF SATURATED WATER ... 0.13833E-03 KCAL/M·SEC·DEG-C  
 THERMAL CONDUCTIVITY OF SATURATED STEAM ... 0.14222E-04 KCAL/M·SEC·DEG-C  
 ISOBARIC SPECIFIC HEAT CAPASITY OF WATER .. 0.12473E 01 KCAL/KG·DEG-C  
 PRANDTL NUMBER OF SATURATED WATER ..... 0.87512E 00  
 TEMPERATURE OF SUBCOOLED WATER AS A FUNCTION OF ENTHALPY  
 $T = 276.9 - 0.8017 * ( 291.6 - H ) - 0.000995 * ( 291.6 - H )**2$   
 DENSITY OF SUBCOOLED WATER AS A FUNCTION OF ENTHALPY  
 $\text{ROH} = 755.9 + 1.5046 * ( 291.6 - H ) - 0.002675 * ( 291.6 - H )**2$

## \*\* CONSTANTS AT THE CRITICAL POINT \*\*

CRITICAL PRESSURE ..... 225.6 KG/CM\*\*2  
 (3208.2 PSIA )  
 CRITICAL TEMPERATURE ..... 374.2 DEG-C  
 GRAVITATIONAL CONSTANT ..... 9.807 M/SEC\*\*2

## \*\*\* INNER CHANNEL GEOMETRY \*\*\*

GEOMETRICAL TYPE NUMBER .... 1     INDCTC=FULL  
 ( JP-2 7\*7 )

NO.	NAME	HEIGHT(M)	LENGTH(M)	AREA(M2)	EQ.DIA(M)	E/C COEFT.	H·PERIM(M)
		2.0780				0.4038	
1	SUPP	2.1280	0.0500	0.005027	0.0800	0.0	
2	EXPA	2.2110	0.0830	0.006362	0.0900	0.7500	
3	TIE	2.2360	0.0250	0.008339	0.0142	0.0	
4	FUEL	3.8940	1.6580	0.008339	0.0142	0.2800	1.8830 .... HEATED DUCT
5	TIE	3.9415	0.0475	0.008339	0.0142	0.1064	

SPACER DESIGN NO.	HEIGHT	E/C COEFT.	DUCT	REGION
1	2.7680	0.5260	4	3
2	3.3080	0.5260	4	6

GEOMETRICAL TYPE NUMBER .... 2     INDCTC=FULL  
 ( LEAKAGE )

NO.	NAME	HEIGHT(M)	LENGTH(M)	AREA(M2)	EQ.DIA(M)	E/C COEFT.	H·PERIM(M)
		2.0780				0.6742	
1	SUP1	2.1090	0.0310	0.089600	0.0380	0.2569	
2	SUP2	2.1280	0.0190	0.048640	0.0280	0.6468	
3	FUEL	3.9415	1.8135	0.248500	0.0148	0.4913	0.0 .... HEATED DUCT

NO DATUM ABOUT SPACER

\* AASSY(ASSEMBLY PART AREA) = 0.6004 M\*\*2  
 \* ALEAK(LEAKAGE PART AREA) = 0.2485 M\*\*2  
 \* ACORE(HEATED ZONE TOTAL AREA) = 0.8489 M\*\*2

\*\*\* NORMALIZED HEAT DISTRIBUTION \*\*\*  
( INPUT MODE .... EACH )

	N= 1	N= 2	N= 3	N= 4	N= 5	N= 6	N= 7	N= 8	N= 9	N=10	N=11
SS(N)	1.0000	1.0000	1.0000	1.0000	1.0000	1.0000	1.0000	1.0000	1.0000	1.0000	1.0000
S(N, 8)	0.3045	0.3045	0.3045	0.3045	0.3045	0.3045	0.3045	0.3045	0.3045	0.3045	0.3045
S(N, 7)	0.8671	0.8671	0.8671	0.8671	0.8671	0.8671	0.8671	0.8671	0.8671	0.8671	0.8671
S(N, 6)	1.2977	1.2977	1.2977	1.2977	1.2977	1.2977	1.2977	1.2977	1.2977	1.2977	1.2977
S(N, 5)	1.5307	1.5307	1.5307	1.5307	1.5307	1.5307	1.5307	1.5307	1.5307	1.5307	1.5307
S(N, 4)	1.5307	1.5307	1.5307	1.5307	1.5307	1.5307	1.5307	1.5307	1.5307	1.5307	1.5307
S(N, 3)	1.2977	1.2977	1.2977	1.2977	1.2977	1.2977	1.2977	1.2977	1.2977	1.2977	1.2977
S(N, 2)	0.8671	0.8671	0.8671	0.8671	0.8671	0.8671	0.8671	0.8671	0.8671	0.8671	0.8671
S(N, 1)	0.3045	0.3045	0.3045	0.3045	0.3045	0.3045	0.3045	0.3045	0.3045	0.3045	0.3045

\*\*\* HEAT BALANCE CALCULATION RESULTS \*\*\*

90.0MW, 905.6KG/SEC

BWR FLOW AND ENTHALPY TABLE

- (1) INLET  
FLOW 905.56 KG/SEC  
ENTHALPY 284.20 KCAL/KG  
DENSITY 766.92 KG/M\*\*3
- (2) OUTLET  
FLOW 905.56 KG/SEC  
(WATER) 865.92  
(STEAM) 39.64  
ENTHALPY 307.95 KCAL/KG  
QUALITY 0.0438  
VOID FR. 0.4179  
DENSITY 453.23 KG/M\*\*3
- (3) STEAM PIPE  
FLOW 37.90 KG/SEC  
ENTHALPY 664.87 KCAL/KG
- (5) FEED WATER  
FLOW 38.84 KG/SEC  
ENTHALPY 102.12 KCAL/KG
- (6) DOWN COMMER 1  
FLOW 867.66 KG/SEC  
(WATER) 865.92  
(STEAM) 1.74  
ENTHALPY 292.35 KCAL/KG  
QUALITY 0.0020  
VOID FR. 0.0366  
DENSITY 729.41 KG/M\*\*3
- (7) DOWN COMMER 2  
FLOW 906.50 KG/SEC  
ENTHALPY 284.20 KCAL/KG  
DENSITY 766.92 KG/M\*\*3
- (8) CLEAN UP FLOW  
FLOW 0.94 KG/SEC  
ENTHALPY 284.20 KCAL/KG  
DENSITY 766.92 KG/M\*\*3

IEND 0

IEND 0

\*\*\*\* CALCULATION SYSTEM \*\*\*\*

NO. OF CHANNELS IN X-DIRECTION .....	5	NO. OF DIVISIONS IN ONE CHANNEL (X) ..	2
NO. OF CHANNELS IN Y-DIRECTION .....	5	NO. OF DIVISIONS IN ONE CHANNEL (Y) ..	2
NO. OF BLOCKS IN Z-DIRECTION .....	8	NO. OF DIVISIONS IN ONE BLOCK (Z) ....	3
NO. OF CHANNELS IN X-Y PLANE .....	11		
NO. OF DIVISIONS IN THE REFLECTOR (X-Y)	1		
NO. OF DIVISIONS IN THE REFLECTOR (Z)	0		
NO. OF CONTROL RODS .....	0		
NO. OF IN-CORE MONITORS .....	0		
NO. OF SPECIAL BLOCKS DIVIDED THINNER	0		

\*\*\*\* GEOMETRY \*\*\*\*

WIDTH OF ONE CHANNEL IN X-DIRECTION	13.6600 CM
WIDTH OF ONE CHANNEL IN Y-DIRECTION	13.6600 CM
LENGTH OF ONE BLOCK IN Z-DIRECTION	18.3375 CM
WIDTH OF THE REFLECTOR (X-Y)	0.1000 CM
THICKNESS OF THE CONTROL RODS	0.0 CM
LENGTH OF THE REFLECTOR (Z)	0.0 CM

CHANNELS POSITION IN X-Y PLANE

```

          BACK
    *****
LEFT *                                     * RIGHT
    * 0 0 0 0 11                          *
    * 0 10 9 7 5                            *
    * 0 9 8 6 4                             *
    * 0 7 6 3 2                             *
    * 11 5 4 2 1                            *
    *****
          FORE
    
```

\*\*\*\* BOUNDARY CONDITIONS \*\*\*\*

LOWER SIDE ..... ANALYTICAL  
 UPPER SIDE ..... ANALYTICAL  
 LEFT SIDE ..... ANALYTICAL  
 RIGHT SIDE ..... ZERO DERIVATIVE  
 BACK SIDE ..... ANALYTICAL  
 FORE SIDE ..... ZERO DERIVATIVE

\*\*\*\* FISSION SPECTRUM \*\*\*\*

NO. OF ENERGY GROUPS .....	3		
FISSION SPECTRUM	0.10000E 01	0.0	0.0

\*\*\*\* CONVERGENCE CRITERIA AND RELAXATION FACTORS \*\*\*\*

CONVERGENCE CRITERIA WHEN CALCULATING SOURCE GUESS

CRITERIA ON EIGENVALUE IN 1-DIM. OUTER IT. 0.010000  
 CRITERIA ON SOURCE DISTR. IN 1-DIM. OUTER IT. 0.010000  
 CRITERIA IN 2 - DIMENSIONAL INNER IT. 0.010000  
 CRITERIA IN 2 - DIMENSIONAL OUTER IT. 0.010000  
 MAX. ITERATION TIMES IN 2-DIM. INNER IT. 50  
 MAX. ITERATION TIMES IN 2-DIM. OUTER IT. 50  
 OVER RELAXATION FACTOR OF 1-DIM. OUTER IT. 0.800000  
 OVER RELAXATION FACTOR OF 2-DIM. INNER IT. 1.400000  
 SLOR METHOD IN 2-DIM. INNER IT. IS APPLIED TO ONLY X - AXIS

CONVERGENCE CRITERIA WHEN CALCULATING 3-DIMENSIONAL SYNTHESIS

TEMPORARY CRITERIA OF 3-DIM. INNER IT. WHEN OUTER IT. TIMES ARE LESS THAN 3  
 AND LINK IT. TIMES ARE LESS THAN 2 ..... 0.005000  
 TEMPORARY CRITERIA OF 3-DIM INNER IT. WHEN OUTER IT. TIMES ARE LESS THAN 5  
 AND LINK IT. TIMES ARE LESS THAN 2 ..... 0.003000  
 FINAL CRITERIA OF 3-DIM INNER IT. .... 0.001000  
 MAX. ITERATION TIMES IN 3-DIM. INNER IT. 100  
 MAX. ITERATION TIMES IN 3-DIM. OUTER IT. 30  
 TEMPORARY CRITERIA OF 3-DIM OUTER IT. WHEN LINK IT. TIMES ARE LESS THAN 3 ..... 0.005000  
 TEMPORARY CRITERIA OF 3- DIM OUTER IT. WHEN LINK IT. TIMES ARE LESS THAN 5 ..... 0.003000  
 FINAL CONVERGENCE CRITERIA OF 3-DIM OUTER ITERATION ..... 0.001000  
 RELAXATION FACTOR OF L-XY IN INNER IT. 0.0  
 RELAXATION FACTOR OF L-Z IN INNER IT. 0.0  
 RELAXATION FACTOR IN 3-DIM. OUTER IT. 1.500000

\*\*\* YOUR CALCULATIONAL SYSTEM IS PROPER \*\*\*

NO. OF (A) IS UNDER THE LIMIT BY 16826 WORDS

\*\*\* YOUR CALCULATIONAL SYSTEM IS PROPER \*\*\*

NO. OF (NA) IS UNDER THE LIMIT BY 4852 WORDS

MATERIAL MAP --- BLOCK NO. 0---

```

X 0 1 2 3 4 5 6 7 8 9 10 11
Y
0 *****
  *12 12 12 12 12 12 12 12 12 12 12*
1 *
  *12 12 12 12 12 12 12 12 12*11 11*
2 *
  *12 12 12 12 12 12 12 12 12*11 11*
3 *
  *12 12 12*10 10* 9 9* 7 7* 5 5*
4 *
  *12 12 12*10 10* 9 9* 7 7* 5 5*
5 *
  *12 12 12* 9 9* 8 8* 6 6* 4 4*
6 *
  *12 12 12* 9 9* 8 8* 6 6* 4 4*
7 *
  *12 12 12* 7 7* 6 6* 3 3* 2 2*
8 *
  *12 12 12* 7 7* 6 6* 3 3* 2 2*
9 *
  *12*11 11* 5 5* 4 4* 2 2* 1 1*
10 *
  *12*11 11* 5 5* 4 4* 2 2* 1 1*
11 *****
    
```

SOURCE IT. OF 2-DIM. FOR SOURCE GUESS

	SOURCE IT.	MAX LAMBDA	LAMBDA	MIN LAMBDA	ACC. PARAMETER USED
1	0.12969215E 01	0.10757099E 01	0.75232726E 00	0.0	
2	0.11748936E 01	0.10733767E 01	0.90317586E 00	0.0	
	THETA VALUE	0.33668E-01	0.14196E-57	0.13242E-17	0.15449E-11 0.38427E-05
3	0.11644045E 01	0.10821640E 01	0.95152529E 00	0.38667962E-01	
	THETA VALUE	0.34857E 01	0.12649E 01	0.33216E 00	0.31721E-01 0.38427E-05
4	0.12663551E 01	0.11055897E 01	0.10712258E 01	0.34857262E 01	
5	0.11307456E 01	0.11076285E 01	0.10750822E 01	0.12648881E 01	
6	0.11097576E 01	0.11066328E 01	0.10963507E 01	0.33215947E 00	

FLUX AND SOURCE DISTRIBUTION

EIGEN VALUE

1.0816053

CHANNEL NO.	SOURCE	FLUX-1G	FLUX-2G	FLUX-3G
CHANNEL NO. 1	SOURCE	FLUX-1G	FLUX-2G	FLUX-3G
BLOCK NO. 1	0.18897E 01	0.32545E 02	0.15840E 02	0.15570E 02
2	0.23826E 01	0.57553E 02	0.27749E 02	0.24901E 02
3	0.23645E 01	0.62961E 02	0.30256E 02	0.24600E 02
4	0.18862E 01	0.55708E 02	0.26555E 02	0.24670E 02
5	0.14090E 01	0.43702E 02	0.20139E 02	0.14588E 02
6	0.97802E 00	0.31382E 02	0.14824E 02	0.10104E 02
7	0.61354E 00	0.20063E 02	0.09564E 01	0.63296E 01
8	0.32140E 00	0.99122E 01	0.46692E 01	0.33853E 01
CHANNEL NO. 2	SOURCE	FLUX-1G	FLUX-2G	FLUX-3G
BLOCK NO. 1	0.13744E 01	0.29538E 02	0.14572E 02	0.14395E 02
2	0.22404E 01	0.53090E 02	0.25704E 02	0.23322E 02
3	0.22460E 01	0.58864E 02	0.28238E 02	0.23373E 02
4	0.18179E 01	0.21242E 02	0.24890E 02	0.18899E 02
5	0.13872E 01	0.41026E 02	0.19449E 02	0.13964E 02
6	0.93408E 00	0.29420E 02	0.13925E 02	0.96646E 01
7	0.58487E 00	0.18794E 02	0.88769E 01	0.60423E 01
8	0.30484E 00	0.92621E 01	0.43702E 01	0.32119E 01
CHANNEL NO. 3	SOURCE	FLUX-1G	FLUX-2G	FLUX-3G
BLOCK NO. 1	0.12638E 01	0.27359E 02	0.13318E 02	0.13214E 02
2	0.20787E 01	0.48768E 02	0.25623E 02	0.21644E 02
3	0.21169E 01	0.54483E 02	0.26159E 02	0.22034E 02
4	0.11244E 01	0.48898E 02	0.21198E 02	0.17958E 02
5	0.12827E 01	0.38239E 02	0.18204E 02	0.13316E 02
6	0.88874E 00	0.27432E 02	0.13012E 02	0.92095E 01
7	0.55540E 00	0.17511E 02	0.87883E 01	0.37561E 01
8	0.28827E 00	0.86097E 01	0.40713E 01	0.30390E 01
CHANNEL NO. 4	SOURCE	FLUX-1G	FLUX-2G	FLUX-3G
BLOCK NO. 1	0.11423E 01	0.24620E 02	0.11984E 02	0.11941E 02
2	0.19045E 01	0.44135E 02	0.21238E 02	0.19823E 02
3	0.18243E 01	0.35348E 02	0.24890E 02	0.20477E 02
4	0.16245E 01	0.44483E 02	0.21350E 02	0.16936E 02
5	0.12076E 01	0.35130E 02	0.16753E 02	0.12548E 02
6	0.83599E 00	0.25207E 02	0.11980E 02	0.86725E 01
7	0.52228E 00	0.16085E 02	0.76270E 01	0.51118E 01
8	0.26970E 00	0.78905E 01	0.37412E 01	0.28436E 01
CHANNEL NO. 5	SOURCE	FLUX-1G	FLUX-2G	FLUX-3G
BLOCK NO. 1	0.81707E 00	0.17027E 02	0.82750E 01	0.85824E 01
2	0.14043E 01	0.30970E 02	0.14887E 02	0.14705E 02
3	0.15164E 01	0.35348E 02	0.17058E 02	0.15875E 02
4	0.13082E 01	0.32305E 02	0.15533E 02	0.13699E 02
5	0.99371E 00	0.25779E 02	0.12342E 02	0.10408E 02
6	0.49032E 00	0.18563E 02	0.88636E 01	0.72341E 01
7	0.42886E 00	0.11845E 02	0.56421E 01	0.45066E 01
8	0.21609E 00	0.57698E 01	0.27459E 01	0.23164E 01
CHANNEL NO. 6	SOURCE	FLUX-1G	FLUX-2G	FLUX-3G
BLOCK NO. 1	0.10345E 01	0.22210E 02	0.10809E 02	0.10814E 02
2	0.17397E 01	0.40503E 02	0.19378E 02	0.18112E 02
3	0.18243E 01	0.45115E 02	0.21770E 02	0.18982E 02
4	0.13297E 01	0.40788E 02	0.19585E 02	0.15908E 02
5	0.11386E 01	0.32306E 02	0.15631E 02	0.11838E 02
6	0.78925E 00	0.25207E 02	0.11945E 02	0.81849E 01
7	0.49190E 00	0.14801E 02	0.70290E 01	0.51026E 01
8	0.25261E 00	0.72418E 01	0.34392E 01	0.26631E 01
CHANNEL NO. 7	SOURCE	FLUX-1G	FLUX-2G	FLUX-3G
BLOCK NO. 1	0.78691E 00	0.14332E 02	0.65644E 01	0.65455E 01
2	0.14043E 01	0.26135E 02	0.12658E 02	0.14712E 02
3	0.15022E 01	0.24993E 02	0.14479E 02	0.16183E 02
4	0.13169E 01	0.27535E 02	0.13250E 02	0.14247E 02
5	0.10122E 01	0.22043E 02	0.10588E 02	0.10995E 02
6	0.70832E 00	0.18902E 02	0.78037E 01	0.77248E 01
7	0.44326E 00	0.10151E 02	0.48443E 01	0.48448E 01
8	0.22382E 00	0.49478E 01	0.23586E 01	0.24715E 01
CHANNEL NO. 8	SOURCE	FLUX-1G	FLUX-2G	FLUX-3G
BLOCK NO. 1	0.82195E 00	0.17541E 02	0.85324E 01	0.85952E 01
2	0.14043E 01	0.24891E 02	0.12658E 02	0.14680E 02
3	0.15146E 01	0.36423E 02	0.17592E 02	0.15817E 02
4	0.13078E 01	0.33278E 02	0.16017E 02	0.13607E 02
5	0.99079E 00	0.26533E 02	0.12728E 02	0.10297E 02
6	0.48757E 00	0.16152E 02	0.42377E 01	0.47148E 01
7	0.42789E 00	0.12195E 02	0.48443E 01	0.44465E 01
8	0.21715E 00	0.59344E 01	0.28295E 01	0.22877E 01
CHANNEL NO. 9	SOURCE	FLUX-1G	FLUX-2G	FLUX-3G
BLOCK NO. 1	0.80767E 00	0.10713E 02	0.51997E 01	0.65559E 01
2	0.10781E 01	0.19706E 02	0.92290E 01	0.11620E 02
3	0.12069E 01	0.22847E 02	0.11013E 02	0.13038E 02
4	0.10800E 01	0.21141E 02	0.40180E 02	0.11705E 02
5	0.84380E 00	0.17049E 02	0.84331E 01	0.91717E 01
6	0.59632E 00	0.12340E 02	0.59139E 01	0.65030E 01
7	0.37521E 00	0.78865E 01	0.37737E 01	0.40967E 01
8	0.18769E 00	0.38255E 01	0.18289E 01	0.20667E 01
CHANNEL NO. 10	SOURCE	FLUX-1G	FLUX-2G	FLUX-3G
BLOCK NO. 1	0.41811E 00	0.62848E 01	0.30482E 01	0.46201E 01
2	0.76251E 00	0.11670E 02	0.56384E 01	0.83955E 01
3	0.87723E 00	0.13670E 02	0.62979E 01	0.96770E 01
4	0.80521E 00	0.12807E 02	0.61703E 01	0.89052E 01
5	0.69274E 00	0.10410E 02	0.50089E 01	0.71490E 01
6	0.46147E 00	0.75823E 01	0.36432E 01	0.51311E 01
7	0.29267E 00	0.48572E 01	0.23518E 01	0.32401E 01
8	0.14498E 00	0.23477E 01	0.11268E 01	0.16235E 01
CHANNEL NO. 11	SOURCE	FLUX-1G	FLUX-2G	FLUX-3G
BLOCK NO. 1	0.53704E 00	0.84832E 01	0.40950E 01	0.38870E 01
2	0.96452E 00	0.15562E 02	0.75107E 01	0.10565E 02
3	0.10904E 01	0.18077E 02	0.87106E 01	0.11978E 02
4	0.98568E 00	0.16804E 02	0.80834E 01	0.10848E 02
5	0.77633E 00	0.13584E 02	0.65188E 01	0.85971E 01
6	0.53211E 00	0.98545E 01	0.47201E 01	0.61340E 01
7	0.34876E 00	0.63032E 01	0.30151E 01	0.38806E 01
8	0.17386E 00	0.30591E 01	0.14628E 01	0.19473E 01

LEAKAGE DISTRIBUTION

CHANNEL NO.	1						POWER
BLOCK NO.	LZ-1G	LZ-2G	LZ-3G	LXY-1G	LXY-2G	LXY-3G	
1	0.30735E-02	0.45987E-03	-0.38026E-03	0.13511E-02	0.72141E-03	0.27355E-03	0.14901E 01
2	0.17776E-02	0.89658E-03	0.63030E-03	0.15472E-02	0.69009E-03	0.17644E-03	0.23924E 01
3	0.11504E-02	0.58763E-03	0.26464E-03	0.13526E-02	0.64537E-03	-0.21490E-03	0.23632E 01
4	0.49215E-03	0.22465E-03	-0.96859E-04	0.15031E-02	0.61397E-03	0.31984E-04	0.18944E 01
5	0.49352E-04	0.43300E-05	-0.12581E-03	0.14715E-02	0.65310E-03	0.18045E-04	0.14072E 01
6	-0.18992E-03	-0.11356E-03	-0.13901E-03	0.14793E-02	0.64732E-03	0.52516E-04	0.97661E 00
7	-0.36215E-03	-0.19771E-03	-0.19469E-03	0.15076E-02	0.66904E-03	0.67397E-04	0.61240E 00
8	0.16717E-02	-0.29912E-03	-0.30359E-02	0.13533E-02	0.69849E-03	0.15433E-03	0.32103E 00

CHANNEL NO.	2						POWER
BLOCK NO.	LZ-1G	LZ-2G	LZ-3G	LXY-1G	LXY-2G	LXY-3G	
1	0.30076E-02	0.82519E-03	-0.40894E-03	0.16408E-02	0.76390E-03	0.31709E-03	0.13775E 01
2	0.17525E-02	0.87935E-03	0.61193E-03	0.16764E-02	0.72872E-03	0.19473E-03	0.22403E 01
3	0.11509E-02	0.58869E-03	0.28405E-03	0.17904E-02	0.68316E-03	0.10977E-03	0.22499E 01
4	0.13348E-03	0.26980E-03	-0.11937E-04	0.17734E-02	0.76209E-03	0.31984E-04	0.18113E 01
5	0.84673E-04	0.26590E-04	-0.12692E-03	0.16509E-02	0.67159E-03	-0.27299E-04	0.13056E 01
6	-0.18586E-03	-0.11600E-03	-0.13656E-03	0.16489E-02	0.70513E-03	-0.11868E-04	0.93284E 00
7	-0.35736E-03	-0.19143E-03	-0.19499E-03	0.16525E-02	0.71056E-03	0.52428E-04	0.59402E 00
8	0.16478E-02	-0.30117E-03	-0.49263E-02	0.16846E-02	0.77078E-03	0.15940E-03	0.30451E 00

CHANNEL NO.	3						POWER
BLOCK NO.	LZ-1G	LZ-2G	LZ-3G	LXY-1G	LXY-2G	LXY-3G	
1	0.29620E-02	0.80303E-03	-0.43092E-03	0.16880E-02	0.80184E-03	0.36199E-03	0.12645E 01
2	0.17144E-02	0.85500E-03	0.58634E-03	0.17548E-02	0.78729E-03	0.27428E-03	0.26941E 01
3	0.11540E-02	0.58904E-03	0.28690E-03	0.17776E-02	0.64537E-03	0.10977E-03	0.23184E 01
4	0.32445E-03	0.23943E-03	-0.33546E-04	0.18475E-02	0.78478E-03	-0.87535E-04	0.17252E 01
5	0.10304E-03	0.35834E-04	-0.12737E-03	0.18141E-02	0.73332E-03	-0.66954E-04	0.12815E 01
6	-0.17823E-03	-0.11338E-03	-0.13480E-03	0.18114E-02	0.76798E-03	-0.50143E-04	0.86777E 00
7	-0.35361E-03	-0.19808E-03	-0.19300E-03	0.18093E-02	0.77271E-03	0.20433E-04	0.55019E 00
8	0.16494E-02	-0.29463E-03	-0.47979E-02	0.18335E-02	0.82852E-03	0.13816E-03	0.28802E 00

CHANNEL NO.	4						POWER
BLOCK NO.	LZ-1G	LZ-2G	LZ-3G	LXY-1G	LXY-2G	LXY-3G	
1	0.29095E-02	0.78031E-03	-0.46434E-03	0.17744E-02	0.85111E-03	0.41588E-03	0.11426E 01
2	0.16904E-02	0.83745E-03	0.57125E-03	0.17904E-02	0.84495E-03	0.44495E-03	0.19048E 01
3	0.11340E-02	0.58904E-03	0.28690E-03	0.18170E-02	0.64537E-03	0.31107E-03	0.19675E 01
4	0.36535E-03	0.27714E-03	-0.19417E-04	0.19417E-02	0.86797E-03	0.13369E-03	0.16273E 01
5	0.10408E-03	0.29267E-04	-0.13388E-03	0.20087E-02	0.86790E-03	-0.52647E-04	0.12065E 01
6	-0.18699E-03	-0.10263E-03	-0.13531E-03	0.20087E-02	0.87089E-03	-0.31876E-04	0.91101E 00
7	-0.38428E-03	-0.19489E-03	-0.18745E-03	0.20095E-02	0.86747E-03	0.46143E-03	0.52167E 00
8	0.16120E-02	-0.26404E-03	-0.46455E-02	0.20095E-02	0.86247E-03	0.16482E-03	0.26947E 00

CHANNEL NO.	5						POWER
BLOCK NO.	LZ-1G	LZ-2G	LZ-3G	LXY-1G	LXY-2G	LXY-3G	
1	0.27626E-02	0.70911E-03	-0.48656E-03	0.31283E-02	0.10906E-02	-0.13871E-02	0.81742E 00
2	0.16207E-02	0.79091E-03	0.50549E-03	0.32849E-02	0.11409E-02	-0.14095E-02	0.14095E 01
3	0.11254E-02	0.55508E-03	0.28751E-03	0.33401E-02	0.12357E-02	-0.16140E-02	0.15163E 01
4	0.38362E-03	0.28855E-03	0.86658E-04	0.34481E-02	0.13275E-02	-0.18455E-02	0.13080E 01
5	0.15355E-03	0.64415E-04	-0.34398E-04	0.35163E-02	0.13999E-02	-0.17739E-02	0.59357E 00
6	-0.13707E-03	-0.78311E-04	-0.35333E-03	0.35836E-02	0.12933E-02	-0.17339E-02	0.59357E 00
7	-0.30778E-03	-0.16534E-03	-0.16495E-03	0.36489E-02	0.13592E-02	-0.22443E-02	0.42962E 00
8	0.15908E-02	-0.22251E-03	-0.39684E-02	0.35863E-02	0.13661E-02	-0.19991E-02	0.21801E 00

CHANNEL NO.	6						POWER
BLOCK NO.	LZ-1G	LZ-2G	LZ-3G	LXY-1G	LXY-2G	LXY-3G	
1	0.28625E-02	0.75850E-03	-0.48160E-03	0.18119E-02	0.90609E-03	0.41588E-03	0.10346E 01
2	0.16631E-02	0.81898E-03	0.57125E-03	0.18170E-02	0.84495E-03	0.39312E-03	0.17396E 01
3	0.11339E-02	0.56517E-03	0.29127E-03	0.19920E-02	0.99450E-03	0.34927E-03	0.18238E 01
4	0.37503E-03	0.28586E-03	0.53152E-04	0.20510E-02	0.10013E-02	0.29004E-03	0.15287E 01
5	0.12059E-02	0.39999E-04	-0.11943E-03	0.21691E-02	0.99450E-03	-0.12173E-02	0.11316E 01
6	-0.15980E-03	-0.73101E-04	-0.37878E-04	0.22775E-02	0.10011E-02	-0.27796E-03	0.78744E 00
7	-0.35618E-03	-0.18741E-03	-0.18282E-03	0.21437E-02	0.10321E-02	0.11289E-04	0.49134E 00
8	0.15935E-02	-0.25108E-03	-0.44983E-02	0.21500E-02	0.98317E-03	0.20698E-03	0.25240E 00

CHANNEL NO.	7						POWER
BLOCK NO.	LZ-1G	LZ-2G	LZ-3G	LXY-1G	LXY-2G	LXY-3G	
1	0.27270E-02	0.68974E-03	-0.26745E-03	0.10606E-01	0.11208E-02	-0.10304E-01	0.78718E 00
2	0.16035E-02	0.78086E-03	0.47170E-03	0.10238E-01	0.11501E-02	-0.10908E-01	0.13712E 01
3	0.11231E-02	0.55305E-03	0.28035E-03	0.10423E-01	0.12267E-02	-0.11398E-01	0.15059E 01
4	0.39744E-03	0.29606E-03	0.11906E-03	0.10655E-01	0.12889E-02	-0.11882E-01	0.13178E 01
5	0.14605E-03	0.73101E-04	-0.37878E-04	0.12369E-01	0.13835E-02	-0.12505E-01	0.11304E 01
6	-0.12813E-03	-0.12733E-04	-0.94408E-04	0.10040E-01	0.13045E-02	-0.12498E-01	0.70889E 00
7	-0.27820E-03	-0.15354E-03	-0.11792E-03	0.10949E-01	0.12578E-02	-0.13389E-01	0.44340E 00
8	0.16105E-02	-0.22078E-03	-0.31214E-02	0.10998E-01	0.12711E-02	-0.12891E-01	0.22592E 00

CHANNEL NO.	8						POWER
BLOCK NO.	LZ-1G	LZ-2G	LZ-3G	LXY-1G	LXY-2G	LXY-3G	
1	0.27171E-02	0.71551E-03	-0.21929E-03	0.19827E-02	0.10099E-02	0.42681E-03	0.82218E 00
2	0.16097E-02	0.78573E-03	0.50358E-03	0.21106E-02	0.10755E-02	0.31295E-03	0.14095E 01
3	0.11339E-02	0.55833E-03	0.29138E-03	0.21755E-02	0.11645E-02	0.42716E-03	0.15195E 01
4	0.38044E-03	0.28631E-03	0.83965E-04	0.22599E-02	0.22599E-02	0.58975E-03	0.30740E 01
5	0.15300E-03	0.64415E-04	-0.34398E-04	0.22804E-02	0.13313E-02	-0.60180E-03	0.49292E 00
6	-0.13338E-03	-0.77037E-04	-0.12878E-03	0.23803E-02	0.13244E-02	0.40969E-03	0.48715E 00
7	-0.31114E-03	-0.17234E-03	-0.17111E-03	0.24484E-02	0.13167E-02	0.19593E-03	0.42759E 00
8	0.15654E-02	-0.21431E-03	-0.41542E-02	0.24079E-02	0.12389E-02	0.41229E-03	0.21705E 00

CHANNEL NO.	9						POWER
BLOCK NO.	LZ-1G	LZ-2G	LZ-3G	LXY-1G	LXY-2G	LXY-3G	
1	0.26574E-02	0.65575E-03	-0.26782E-03	0.11785E-01	0.12687E-02	-0.12049E-01	0.40836E 00
2	0.15683E-02	0.75907E-03	0.45000E-03	0.11898E-01	0.13418E-02	-0.12395E-01	0.10791E 01
3	0.11071E-02	0.53980E-03	0.27809E-03	0.12109E-01	0.14670E-02	-0.12731E-01	0.12080E 01
4	0.60538E-03	0.24691E-03	0.12420E-03	0.12369E-01	0.15887E-02	-0.13535E-01	0.10808E 01
5	0.18498E-03	0.84540E-04	-0.21178E-03	0.12530E-01	0.16084E-02	-0.13517E-01	0.84438E 00
6	-0.11011E-03	-0.60844E-04	-0.74782E-04	0.12634E-01	0.17409E-02	-0.13829E-01	0.59709E 00
7	-0.29933E-03	-0.14001E-03	-0.98541E-04	0.12656E-01	0.17454E-02	-0.14083E-01	0.37541E 00
8	0.16109E-02	-0.15256E-03	-0.27018E-02	0.12648E-01	0.17057E-02	-0.13709E-01	0.18782E 00

CHANNEL NO.	10						POWER
BLOCK NO.	LZ-1G	LZ-2G	LZ-3G	LXY-1G	LXY-2G	LXY-3G	
1	0.25903E-02	0.62045E-03	-0.89469E-04	0.21641E-01	0.14249E-02	-0.20486E-01	0.41985E 00
2	0.15210E-02	0.73245E-03	0.41435E-03	0.21690E-01	0.15397E-02	-0.20528E-01	0.76376E 00
3	0.10914E-02	0.52631E-03	0.27393E-03	0.21892E-01	0.17480E-02	-0.20655E-01	0.87890E 00
4	0.60649E-03	0.24691E-03	0.13753E-03	0.22294E-01	0.18181E-02	-0.21003E-01	0.80642E 00
5	0.20813E-03	0.97129E-04	0.24415E-04	0.22503E-01	0.20289E-02	-0.21308E-01	0.64366E 00
6	-0.84457E-04	-0.44588E-04	-0.44799E-04	0.22676E-01	0.21153E-02	-0.21552E-01	0.46213E 00
7	-0.23072E-03	-0.12342E-03	-0.67619E-04	0.22733E-01	0.21514E-02	-0.21747E-01	0.29308E 00
8	0.16417E-02	-0.69544E-04	-0.18773E-02	0.22661E-01	0.20617E-02	-0.21359E-01	0.14952E 00

CHANNEL NO.	11						POWER
BLOCK NO.	LZ-1G	LZ-2G	LZ-3G	LXY-1G	LXY-2G	LXY-3G	
1	0.26390E-02	0.64098E-03	-0.11819E-03	0.18657E-01	0.14781E-02	-0.18367E-01	0.33785E 00
2	0.15578E-02	0.75346E-03	0.43075E-03	0.18711E-01	0.15622E-02	-0.18536E-01	0.96392E 00
3	0.10915E-02	0.53061E-03	0.27302E-03	0.18963E-01	0.17035E-02	-0.18883E-01	0.10919E 01
4	0.61115E-03	0.24691E-03	0.13240E-03	0.19199E-01	0.18360E-02	-0.19299E-01	0.98887E 00
5	0.19033E-03	0.89859E-04	0.16462E-04	0			

\*\*\* HEAT DISTRIBUTION (KCAL/SEC) \*\*\*

TOTAL POWER = 90.0 MW = 21500.2 KCAL/SEC  
 LEAK HEAT RATE = 0.0188

	N= 1	N= 2	N= 3	N= 4	N= 5	N= 6	N= 7	N= 8	N= 9	N=10	N=11	N=12
@CHANL	419.63	397.05	373.48	347.01	270.19	322.13	269.90	270.31	219.06	161.63	199.14	404.20
@(N= 8)	11.76	11.15	10.55	9.87	7.98	9.24	8.20	7.95	6.88	5.32	6.38	11.88
@(N= 7)	22.44	21.39	20.33	19.11	15.73	18.00	16.24	15.66	13.75	10.73	12.79	23.23
@(N= 6)	35.77	34.17	32.51	30.59	25.27	28.84	25.96	25.17	21.87	16.93	20.27	37.12
@(N= 5)	51.54	49.28	46.93	44.19	36.38	41.66	37.09	36.27	30.93	23.57	28.49	53.22
@(N= 4)	69.38	66.34	63.19	59.60	47.91	55.99	48.26	47.88	39.59	29.54	36.15	70.33
@(N= 3)	86.55	82.22	77.51	72.06	55.54	66.80	55.06	55.65	44.24	32.19	39.99	83.06
@(N= 2)	87.62	82.05	76.15	69.75	51.44	63.71	50.22	51.61	39.52	27.97	35.38	78.75
@(N= 1)	54.57	50.45	46.31	41.85	29.94	37.89	28.86	30.11	22.28	15.38	19.70	46.62

\*\*\* FLOW AND PRESSURE DROP \*\*\*

	N= 1	N= 2	N= 3	N= 4	N= 5	N= 6	N= 7	N= 8	N= 9	N=10	N=11	N=12
W(N)	10.529	10.636	10.757	10.894	11.414	11.044	11.421	11.413	11.874	12.402	12.041	90.556
DP(N)	2273.1	2272.3	2271.0	2270.1	2266.3	2268.9	2266.3	2266.3	2264.4	2264.0	2264.3	1705.7
DPH(N)	941.0	960.9	983.3	1011.2	1099.7	1037.1	1102.6	1099.2	1179.0	1272.4	1213.3	1422.3
DPL(N)	1332.1	1311.4	1287.7	1258.9	1166.6	1231.8	1163.7	1167.1	1085.4	991.7	1051.1	283.4
DPFR(N)	596.8	584.8	570.0	552.5	488.1	534.4	485.6	488.6	430.9	359.9	407.6	25.0
DPEC(N)	278.8	283.7	289.4	295.8	321.3	303.0	321.6	321.2	344.7	372.9	353.3	258.4
DPSP(N)	195.1	192.8	190.5	187.7	182.2	185.9	181.6	182.3	179.1	176.6	177.3	0.0
DPAC(N)	261.4	250.1	237.8	223.0	175.0	208.5	174.8	175.1	130.7	82.2	112.9	0.0

$$DPAVE = \frac{\sum_{N=1}^{12} DP(N) \cdot W(N) \cdot NO(N)}{\sum_{N=1}^{12} W(N) \cdot NO(N)} = 2267.6$$

\*\*\* CORE AVERAGE VOID FRACTION \*\*\*

$$ALPHA1 = \frac{\sum_{N=1}^{11} \sum_{K=1}^8 \sigma(\alpha(N,K)) \cdot A(N) \cdot NO(N)}{\sum_{N=1}^{11} \sum_{K=1}^8 \sigma(A(N)) \cdot NO(N)} = 0.2666$$

$$ALPHA2 = \frac{\sum_{N=1}^{12} \sum_{K=1}^8 \sigma(\alpha(N,K)) \cdot A(N) \cdot NO(N)}{\sum_{N=1}^{12} \sum_{K=1}^8 \sigma(A(N)) \cdot NO(N)} = 0.1886$$

$$ALPHA3 = \frac{\sum_{N=1}^{11} \sum_{K=1}^8 \sigma(\alpha(N,K)) \cdot @ (N,K) \cdot A(N) \cdot NO(N)}{\sum_{N=1}^{11} \sum_{K=1}^8 \sigma(@CHANL(N)) \cdot A(N) \cdot NO(N)} = 0.2408$$

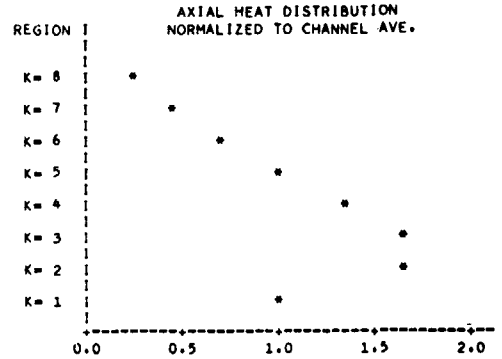
$$ALPHA4 = \frac{\sum_{N=1}^{12} \sum_{K=1}^8 \sigma(\alpha(N,K)) \cdot @ (N,K) \cdot A(N) \cdot NO(N)}{\sum_{N=1}^{12} \sum_{K=1}^8 \sigma(@CHANL(N)) \cdot A(N) \cdot NO(N)} = 0.1533$$



\*\*\* DETAILS OF THE 1-ST ASSEMBLY \*\*\* NO.1

\* CHANNEL HEAT PRODUCT 431.65 KCAL/SEC  
 \* RATE TO CORE AVE. 1.4732

REGION	HEIGHT (M)	HEAT (KC/S)	NORM.TO CHAN.AVE.	NORM.TO CORE AVE.	HEAT FLUX (KC/S.M <sup>2</sup> )	HEAT INTG. (KC/S)
K=8	3.7900	12.16	0.2254	0.3320	35.22	431.65
K=7	3.6066	23.32	0.4322	0.6368	67.54	419.49
K=6	3.4233	37.24	0.6901	1.0167	107.84	396.17
K=5	3.2399	53.71	0.9954	1.4664	155.54	358.93
K=4	3.0565	72.28	1.3397	1.9736	209.34	305.22
K=3	2.8731	89.52	1.6591	2.4442	254.26	232.94
K=2	2.6898	88.91	1.6479	2.4277	257.50	143.42
K=1	2.5064	54.50	1.0102	1.4882	157.85	54.50
K=1	2.3230					0.0

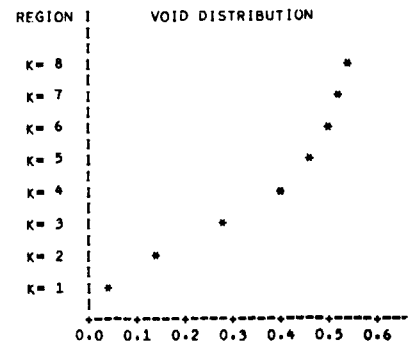


\*\*\* DETAILS OF THE 1-ST ASSEMBLY \*\*\* NO.2

\* COOLANT FLOW 11.760 KG/SEC  
 \* VARIATION FROM INLET TO EXIT

	VELOCITY (M/S)	ENTHALPY (KC/KG)	QUALITY	VOID FR.	DENSITY (KG/M <sup>3</sup> )
OUTLET	3.8371	320.91	0.0785	0.5362	367.53
INLET	1.8388	284.20	0.0	0.0	766.92

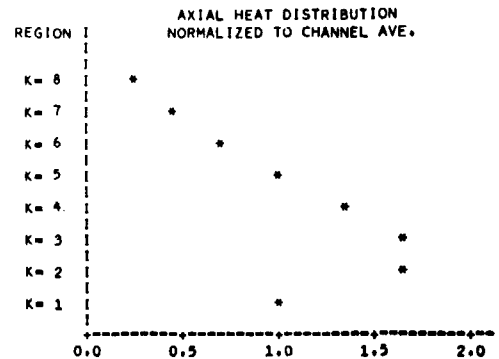
REGION	HEIGHT (M)	ENTHALPY (KC/KG)	QUALITY	VOID FR.	DENSITY (KG/M <sup>3</sup> )	CHFR (JANCEN)	CHFR (HENTI)
K=9	3.7900	320.91	0.07850	0.5362	367.53		
K=8	3.6066	319.87	0.07732	0.5333	369.62	21.4025	20.9515
K=7	3.4233	317.89	0.07334	0.5230	377.05	11.1592	11.0758
K=6	3.2399	314.72	0.06649	0.5037	391.05	6.9892	7.1002
K=5	3.0565	310.16	0.05617	0.4696	415.79	4.8457	5.0061
K=4	2.8731	304.01	0.04179	0.4082	460.22	3.6004	3.7196
K=3	2.6898	296.40	0.02302	0.2868	548.18	2.9072	3.0034
K=2	2.5064	288.84	0.00205	0.1484	647.43	2.9270	3.0240
K=1	2.3230	284.20	0.0	0.0406	734.13	4.7749	4.9330



\*\*\* DETAILS OF THE 2-ND ASSEMBLY \*\*\* NO.1

\* CHANNEL HEAT PRODUCT 405.48 KCAL/SEC  
 \* RATE TO CORE AVE. 1.3839

REGION	HEIGHT (M)	HEAT (KC/S)	NORM.TO CHAN.AVE.	NORM.TO CORE AVE.	HEAT FLUX (KC/S.M <sup>2</sup> )	HEAT INTG. (KC/S)
K=8	3.7900	11.46	0.2260	0.3128	33.18	405.48
K=7	3.6066	22.07	0.4354	0.6026	63.92	394.02
K=6	3.4233	35.30	0.6964	0.9637	102.22	371.95
K=5	3.2399	50.96	1.0054	1.3913	147.58	336.65
K=4	3.0565	68.65	1.3544	1.8743	198.81	285.70
K=3	2.8731	84.23	1.6618	2.2997	243.92	217.05
K=2	2.6898	82.66	1.6309	2.2570	239.40	132.82
K=1	2.5064	50.16	0.9896	1.3695	145.27	50.16
K=1	2.3230					0.0

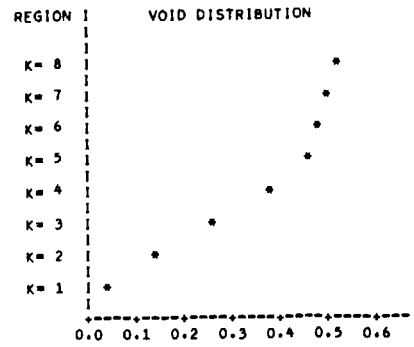


\*\*\* DETAILS OF THE 2-ND ASSEMBLY \*\*\* NO.2

\* COOLANT FLOW 11.680 KG/SEC  
 \* VARIATION FROM INLET TO EXIT

	VELOCITY (M/S)	ENTHALPY (KC/KG)	QUALITY	VOID FR.	DENSITY (KG/M3)
OUTLET	3.7116	318.92	0.0732	0.5226	377.37
INLET	1.8263	284.20	0.0	0.0	766.92

REGION	HEIGHT (M)	ENTHALPY (KC/KG)	QUALITY	VOID FR.	DENSITY (KG/M3)	CHFR (JANCEN)	CHFR (HENT1)
K=9	3.7900	318.92	0.07317	0.5226	377.37		
K=8	3.6066	317.94	0.07206	0.5196	379.53	22.6774	22.6475
K=7	3.4233	316.05	0.06826	0.5089	387.25	11.7725	11.9095
K=6	3.2399	313.03	0.06173	0.4888	401.85	7.3611	7.6111
K=5	3.0565	308.66	0.05188	0.4532	427.65	5.0987	5.2764
K=4	2.8731	302.79	0.03812	0.3864	476.06	3.7848	3.9167
K=3	2.6898	295.58	0.02026	0.2677	562.02	3.0848	3.1922
K=2	2.5064	288.50	0.00053	0.1366	656.74	3.1431	3.2526
K=1	2.3230	284.20	0.0	0.0354	738.20	5.1798	5.3603



\*\*\* CORE MAP OF SOME CHARACTERISTIC VALUES \*\*\*

```

+-----+
|   N   | CHANNEL NUMBER
|  W   | CHANNEL FLOW (KG/SEC)
|  SS  | CHANNEL HEAT RATE TO CORE AVERAGE
| SPEAK(K) | AXIAL PEAKING AND ITS OCCURED REGION
| MCHFR(K) | MCHFR CALCULATED BY JANCEN-LEVY AND ITS REGION
| XCOU | CHANNEL EXIT QUALITY
+-----+
    
```

	1	2	3	4	5
1					11 10.983 0.664 1.605(3) 6.562(3) 0.02761
2	10 10.793 0.537 1.591(3) 8.148(3) 0.01921	9 11.076 0.731 1.614(3) 5.931(3) 0.03200	7 11.244 0.909 1.630(3) 4.743(3) 0.04364	5 11.260 0.912 1.642(3) 4.696(3) 0.04372	
3	9 11.076 0.731 1.614(3) 5.931(3) 0.03200	8 11.263 0.912 1.645(3) 4.686(3) 0.04374	6 11.425 1.100 1.657(3) 3.872(3) 0.05570	4 11.504 1.192 1.661(3) 3.570(3) 0.06150	
4	7 11.244 0.909 1.630(3) 4.743(3) 0.04364	6 11.425 1.100 1.657(3) 3.872(3) 0.05570	3 11.591 1.294 1.663(3) 3.289(3) 0.06782	2 11.680 1.384 1.662(3) 3.085(3) 0.07317	
5	11 10.983 0.664 1.605(3) 6.562(3) 0.02761	5 11.260 0.912 1.642(3) 4.696(3) 0.04372	4 11.504 1.192 1.661(3) 3.570(3) 0.06150	2 11.680 1.384 1.662(3) 3.085(3) 0.07317	1 11.760 1.473 1.659(3) 2.907(3) 0.07850

GROSS PEAKING 2.444 ( 1-ST ASSEMBLY\* 3-RD REGION )  
 MCHFR 2.907 ( 1-ST ASSEMBLY\* 3-RD REGION )

\*\*\*\* CHANNEL NO. 1 \*\*\*\*

Z= DIRECTIONAL FLUX DISTRIBUTION

POSITION	SOURCE	1G-FLUX	2G-FLUX	3G-FLUX
1	3.056250	0.1012370E 01	0.2077612E 02	0.1020599E 02
2	9.168750	0.1502148E 01	0.3316830E 02	0.1610036E 02
3	15.281250	0.1954607E 01	0.4368959E 02	0.2121302E 02
4	21.393750	0.2192270E 01	0.5212941E 02	0.2521374E 02
5	27.506250	0.2427218E 01	0.5810175E 02	0.2811167E 02
6	33.618751	0.2558390E 01	0.6188822E 02	0.2992285E 02
7	39.731251	0.2414591E 01	0.6362971E 02	0.3057949E 02
8	45.843751	0.2381997E 01	0.6344449E 02	0.3049089E 02
9	51.956251	0.2296935E 01	0.6179407E 02	0.2969689E 02
10	58.068751	0.2035030E 01	0.5925799E 02	0.2825370E 02
11	64.181252	0.1898301E 01	0.5586347E 02	0.2663022E 02
12	70.293751	0.1755390E 01	0.5200194E 02	0.2478254E 02
13	76.406250	0.1552687E 01	0.4797459E 02	0.2274290E 02
14	82.518749	0.1407872E 01	0.4377243E 02	0.2074292E 02
15	88.631248	0.1266590E 01	0.3953756E 02	0.1873236E 02
16	94.743748	0.1106475E 01	0.3539939E 02	0.1672236E 02
17	100.856247	0.9760290E 00	0.3134052E 02	0.1480402E 02
18	106.968746	0.8515428E 00	0.2740052E 02	0.1294521E 02
19	113.081245	0.7240794E 00	0.2383445E 02	0.1114373E 02
20	119.193745	0.6117442E 00	0.2001630E 02	0.9434296E 01
21	125.306244	0.5047861E 00	0.1653494E 02	0.7791066E 01
22	131.418743	0.4005117E 00	0.1318614E 02	0.6202209E 01
23	137.531242	0.3093728E 00	0.9935680E 01	0.4664056E 01
24	143.643742	0.2543072E 00	0.6614776E 01	0.3142280E 01

\*\*\*\* CHANNEL NO. 2 \*\*\*\*

Z= DIRECTIONAL FLUX DISTRIBUTION

POSITION	SOURCE	1G-FLUX	2G-FLUX	3G-FLUX
1	3.056250	0.9329858E 00	0.1906940E 02	0.9367611E 01
2	9.168750	0.1387789E 01	0.3099684E 02	0.1480473E 02
3	15.281250	0.1810526E 01	0.4024820E 02	0.1954433E 02
4	21.393750	0.2045750E 01	0.4812522E 02	0.2326339E 02
5	27.506250	0.2272278E 01	0.5377586E 02	0.2603764E 02
6	33.618751	0.2403036E 01	0.5736911E 02	0.2778645E 02
7	39.731251	0.2287208E 01	0.5917444E 02	0.2847868E 02
8	45.843751	0.2263265E 01	0.5912179E 02	0.2845943E 02
9	51.956251	0.2187450E 01	0.5769674E 02	0.2776926E 02
10	58.068751	0.1943237E 01	0.5541068E 02	0.2645448E 02
11	64.181252	0.1815377E 01	0.5229714E 02	0.2496284E 02
12	70.293751	0.1680033E 01	0.4871941E 02	0.2325278E 02
13	76.406250	0.1484310E 01	0.4496737E 02	0.2136521E 02
14	82.518749	0.1346155E 01	0.4103848E 02	0.1949556E 02
15	88.631248	0.1211025E 01	0.3707087E 02	0.1760711E 02
16	94.743748	0.1057037E 01	0.3318748E 02	0.1571160E 02
17	100.856247	0.9321789E 00	0.2938159E 02	0.1390637E 02
18	106.968746	0.8130344E 00	0.2569076E 02	0.1215789E 02
19	113.081245	0.6905889E 00	0.2215181E 02	0.1046480E 02
20	119.193745	0.5831592E 00	0.1875015E 02	0.8856458E 01
21	125.306244	0.4808521E 00	0.1547959E 02	0.7309304E 01
22	131.418743	0.3809013E 00	0.1233434E 02	0.5812151E 01
23	137.531242	0.2935634E 00	0.9282722E 01	0.4365158E 01
24	143.643742	0.2400443E 00	0.6169131E 01	0.2934265E 01